# Mössbauer Spectroscopy

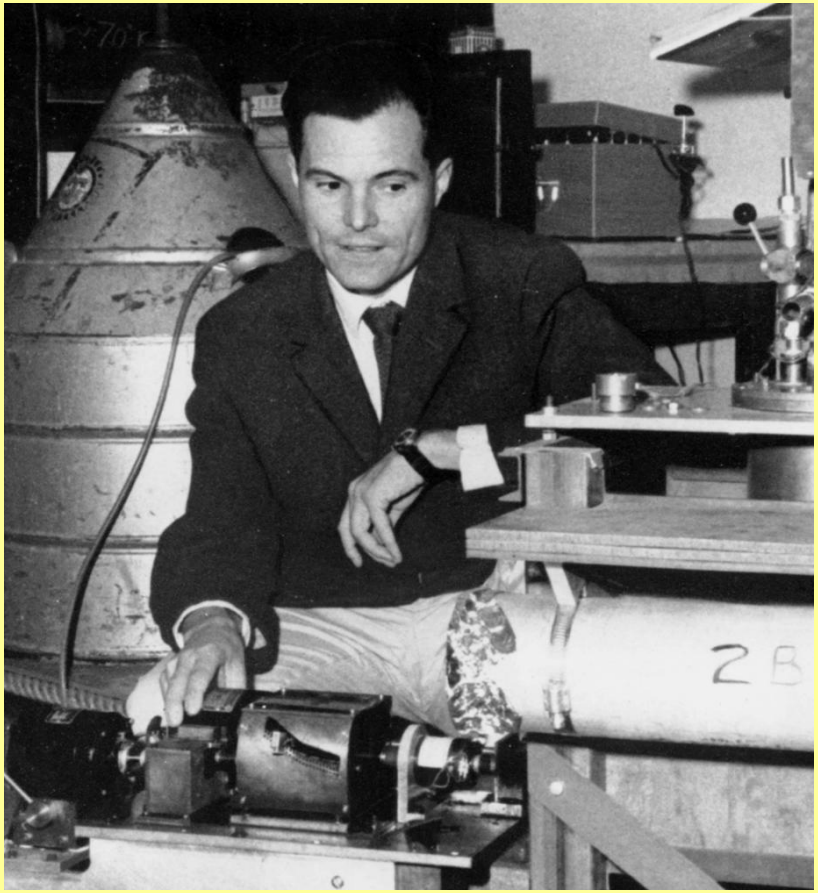

**Rudolf L. Mössbauer**
1929 - 2011

**1958**
**Recoilless Nuclear Resonance Absorption of Gamma-Radiation**

**= the Mössbauer Effect (during PhD)**

**1961**
**Nobel Prize in Physics**

The Mössbauer resonance line is extremely narrow and allows hyperfine interactions to be resolved and evaluated, quadrupole splitting and an isomer shift

# The Mössbauer Effect

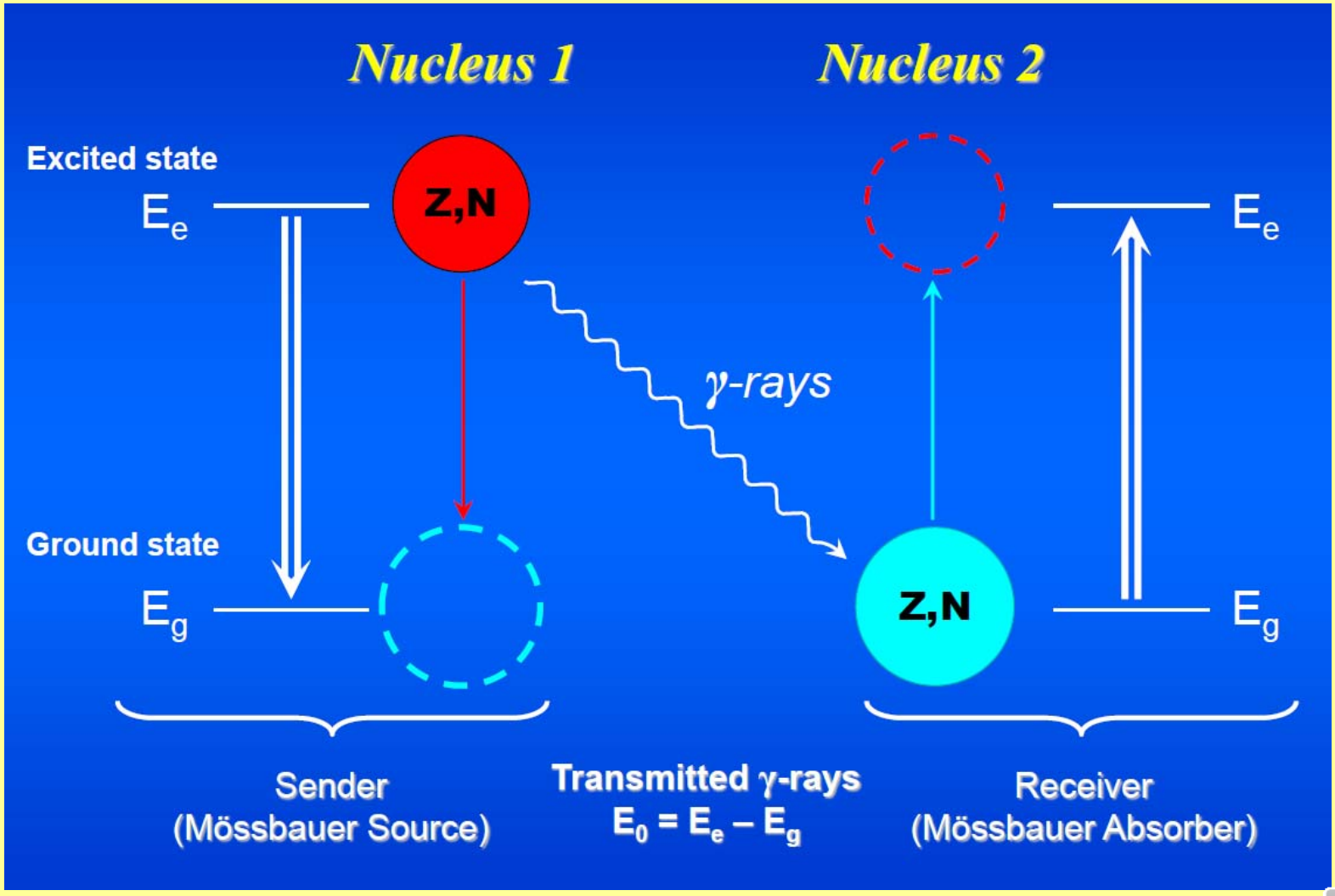

# Recoilless Nuclear Resonance Absorption and Fluorescence of γ-Radiation

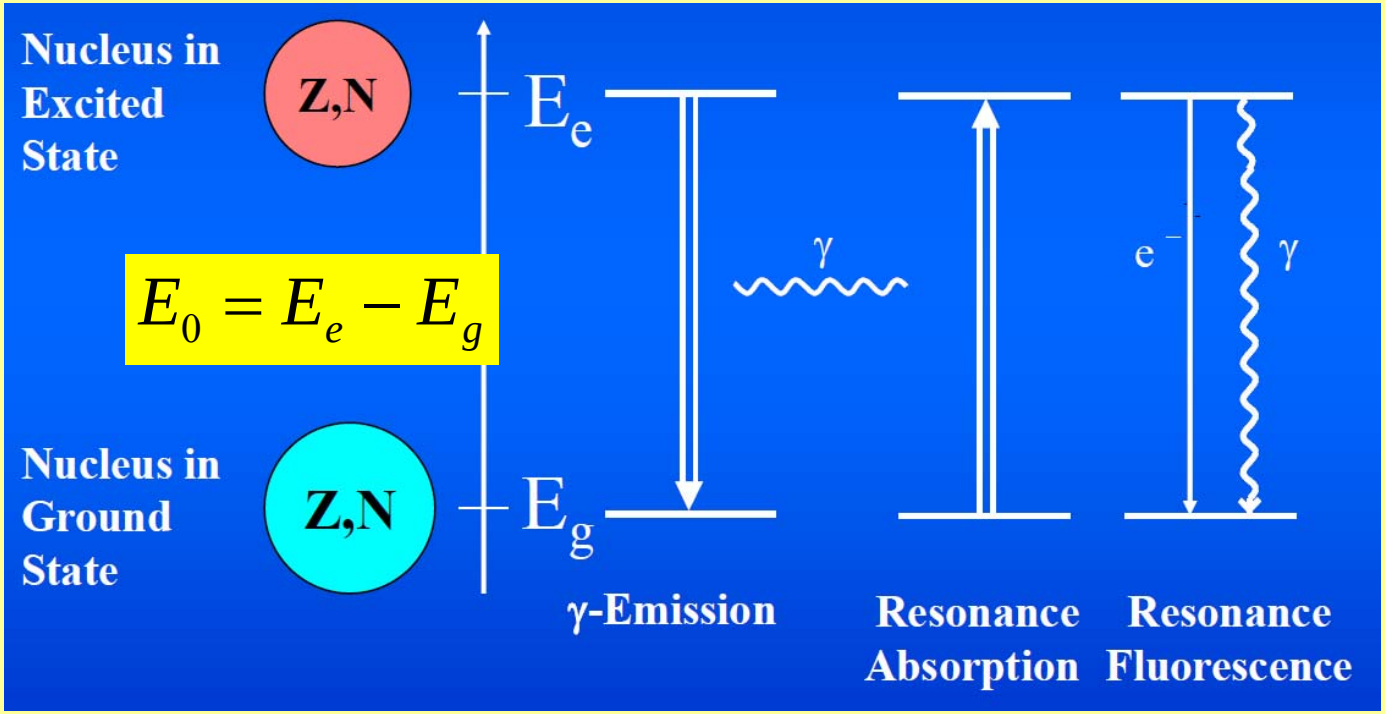


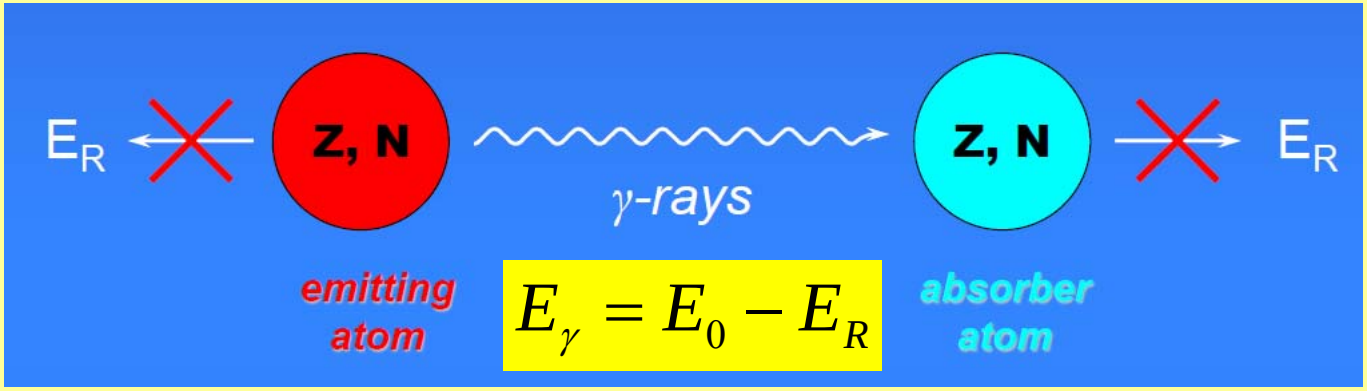


Problem !!!

$$E_\gamma \neq E_0$$

**RECOIL**

Conservation of momentun

$$E_R = \frac{E_\gamma^2}{2mc^2}$$

*m* = nucleus mass

# Mössbauer Active Elements

**Conditions for nuclides to be suitable for Mössbauer spectroscopy:**

- Excited nuclear state lifetimes **$10^{-6}$ - $10^{-11}$ s**

Longer (shorter) lifetimes = too narrow (broad) emission and absorption lines, no effective overlap

- Transition energies **5 - 180 keV**

Transition energies > 180 keV = too large recoil, < 5 keV = absorbed in the source and absorber material

The Mössbauer effect detected in 80 isotopes of 50 elements,
only 20 elements studied in practice Fe, Sn, Sb, Te, I, Au, Ni, Ru, Ir, W, Kr, Xe, rare earth elements, Np. More than 70 % of publications refer to **$^{57}$Fe**

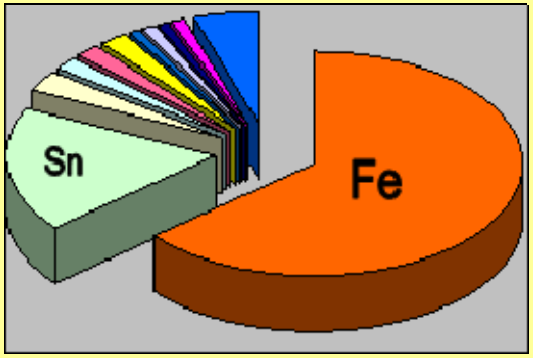


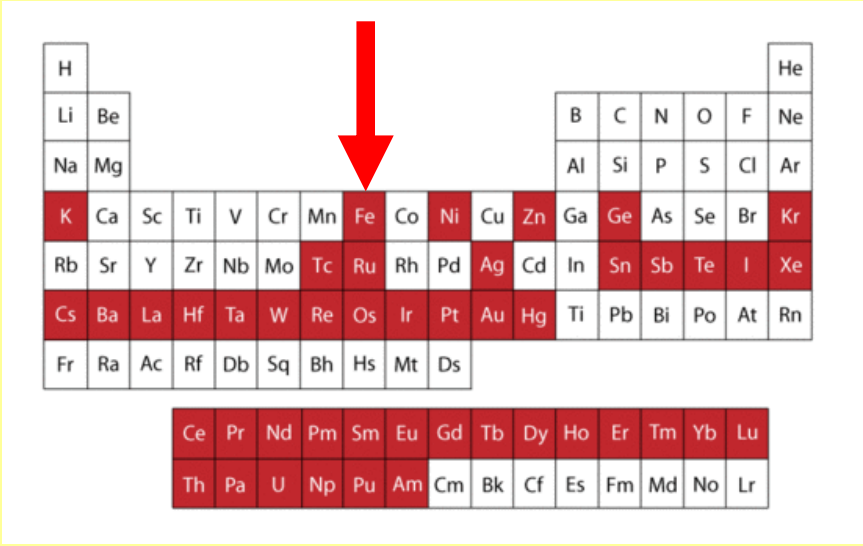

# Nuclear Parameters for Selected Mössbauer Isotopes

| Isotope | $E_\gamma$/keV | Linewidth $\Gamma_r/(\text{mm s}^{-1}) = 2\,\Gamma_{nat}$ | Nuclear spin $I_g$ | $I_e$ | α | Natural abundance % | Nuclear decay* |
|---|---|---|---|---|---|---|---|
| $^{57}$Fe | 14.41 | 0.192 | 1/2– | 3/2– | 8.17 | 2.17 | $^{57}$Co(EC 270 d) |
| $^{61}$Ni | 67.40 | 0.78 | 3/2– | 5/2– | 0.12 | 1.25 | $^{61}$Co(β⁻99 m) |
| $^{119}$Sn | 23.87 | 0.626 | 1/2+ | 3/2+ | 5.12 | 8.58 | $^{119m}$Sn(IT 50 d) |
| $^{121}$Sb | 37.15 | 2.1 | 5/2+ | 7/2+ | ~10 | 57.25 | $^{121m}$Sn(β⁻76 y) |
| $^{125}$Te | 35.48 | 5.02 | 1/2+ | 3/2+ | 12.7 | 6.99 | $^{125}$I(EC 60d) |
| $^{127}$I | 57.60 | 2.54 | 5/2+ | 7/2+ | 3.70 | 100 | $^{127m}$Te (β⁻109 d) |
| $^{129}$I | 27.72 | 0.59 | 7/2+ | 5/2+ | 5.3 | nil | $^{129m}$Te (β⁻33 d) |
| $^{149}$Sm | 22.5 | 1.60 | 7/2– | 5/2– | ~12 | 13.9 | $^{149}$Eu(EC 106 d) |
| $^{151}$Eu | 21.6 | 1.44 | 5/2+ | 7/2+ | 29 | 47.8 | $^{151}$Gd(EC 120 d) |
| $^{161}$Dy | 25.65 | 0.37 | 5/2+ | 5/2– | ~2.5 | 18.88 | $^{161}$Tb(β⁻6.9 d) |
| $^{193}$Ir | 73.0 | 0.60 | 3/2+ | 1/2+ | ~6 | 61.5 | $^{193}$Os(β⁻31 h) |
| $^{197}$Au | 77.34 | 1.87 | 3/2+ | 1/2+ | 4.0 | 100 | $^{197}$Pt(β⁻18 h) |
| $^{237}$Np | 59.54 | 0.067 | 5/2+ | 5/2– | 1.06 | nil | $^{241}$Am(α458 y) |

EC = electron capture, β⁻= beta-decay, IT = isomeric transition, α = alpha-decay

# Nuclear Parameters for Selected Mössbauer Isotopes

| Nuclide | $E_0$ (keV) | $\tau_0$(ns) | $a$(%) | $I_g$ | $I_e$ | $\alpha$ | $\sigma_n$/kbarn | $\sigma_n/\sigma_{ph}$ |
|---|---|---|---|---|---|---|---|---|
| $^{187}$Os | 9.777 | 3.43 | 1.6 | $1/2^-$ | $3/2^-$ | 264. | 194.4 | 5.84 |
| $^{57}$Fe | 14.4129 | 141. | 2.14 | $1/2^-$ | $3/2^-$ | 8.18 | 2464.0 | 428.58 |
| $^{151}$Eu | 21.5412 | 14.0 | 47.8 | $5/2^+$ | $7/2^+$ | 28.0 | 242.6 | 29.06 |
| $^{149}$Sm | 22.5015 | 10.3 | 13.8 | $7/2^-$ | $5/2^+$ | 29.2 | 120.1 | 17.29 |
| $^{119}$Sn | 23.8793 | 25.6 | 8.58 | $1/2^+$ | $3/2^+$ | 5.22 | 1380.5 | 562.59 |
| $^{125}$Te | 35.4920 | 2.14 | 6.99 | $1/2^+$ | $3/2^+$ | 14.0 | 259.0 | 44.11 |
| $^{121}$Sb | 37.1292 | 4.99 | 57.3 | $5/2^+$ | $7/2^+$ | 11.11 | 195.4 | 40.26 |
| $^{129}$Xe | 39.5813 | 1.47 | 26.4 | $1/2^+$ | $3/2^+$ | 12.31 | 234.7 | 47.24 |
| $^{61}$Ni | 67.408 | 7.60 | 1.19 | $3/2^-$ | $5/2^-$ | 0.139 | 709.1 | 7046. |
| $^{73}$Ge | 68.752 | 2.51 | 7.76 | $9/2^+$ | $7/2^+$ | 0.227 | 337.5 | 2121. |
| $^{197}$Au | 77.351 | 2.76 | 100. | $3/2^+$ | $1/2^+$ | 4.36 | 38.1 | 56.22 |
| $^{191}$Ir | 82.407 | 5.89 | 37.3 | $3/2^+$ | $1/2^+$ | 10.9 | 15.1 | 6.20 |
| $^{155}$Gd | 86.546 | 9.13 | 14.7 | $3/2^-$ | $5/2^+$ | 0.434 | 341.7 | 304.61 |
| $^{99}$Ru | 89.571 | 28.8 | 12.7 | $5/2^+$ | $3/2^+$ | 1.498 | 81.2 | 315.04 |

$\tau_0$ = mean lifetime of exited state, $a$(%) = natural abundance, $\alpha$ = alpha-decay

# Nuclear Decay Scheme for $^{57}$Fe Mössbauer Resonance

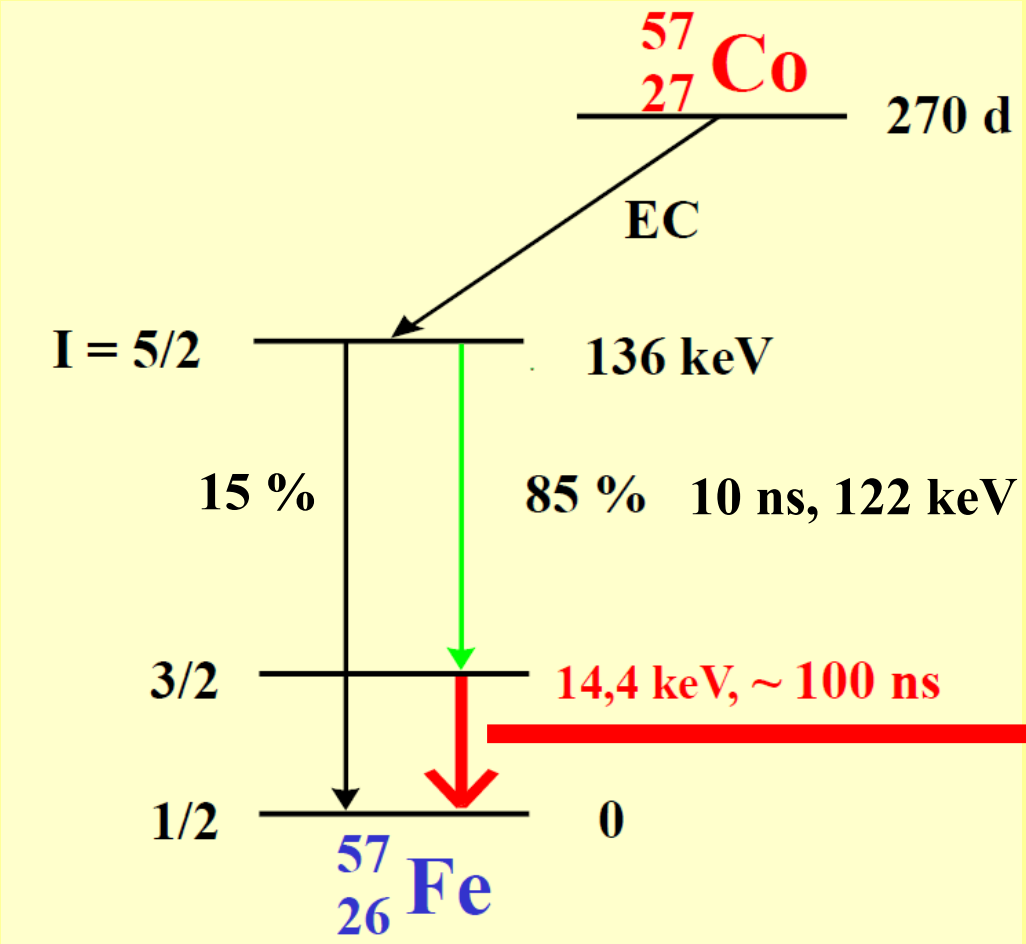


Radioactive $^{57}$Co (halflife 270 d) is generated in a cyclotron and diffused into Rh

$^{57}$Co serves as the gamma radiation source for $^{57}$Fe Mössbauer spectroscopy

$^{57}$Fe - 2 at.% natural abundance

**Mössbauer Emission**

# Nuclear Resonance Absorption

Energy decay of the absorber nucleus to ground state

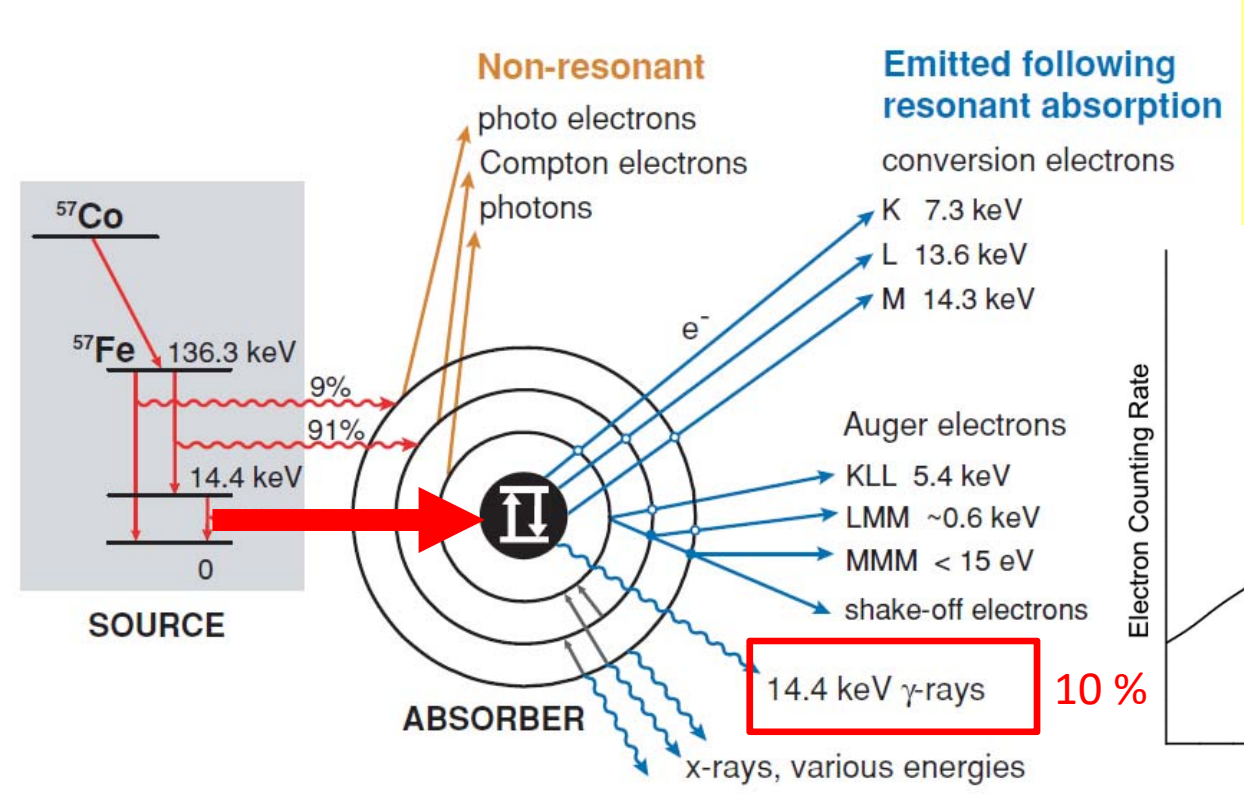


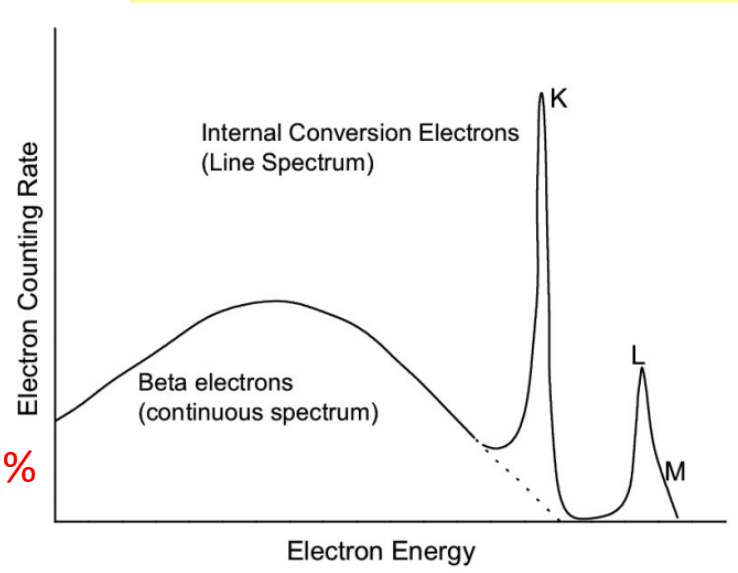

# $^{57}$Fe Mössbauer Source

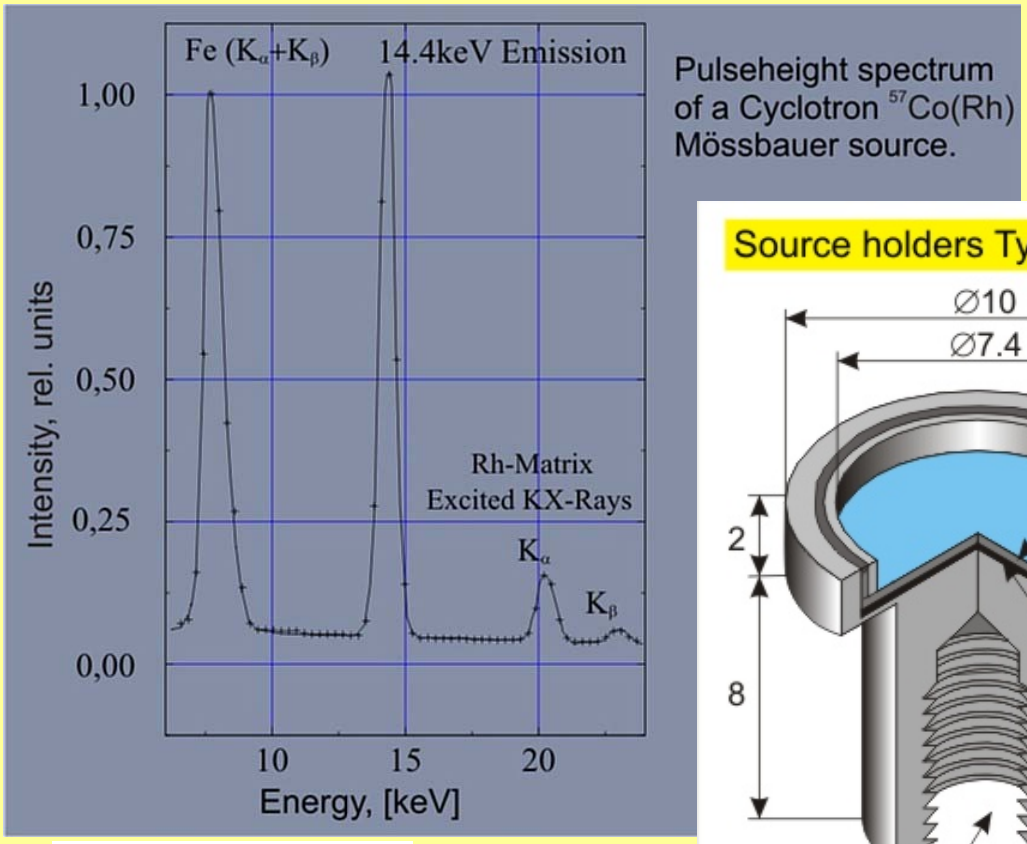


Pulseheight spectrum of a Cyclotron $^{57}$Co(Rh) Mössbauer source.

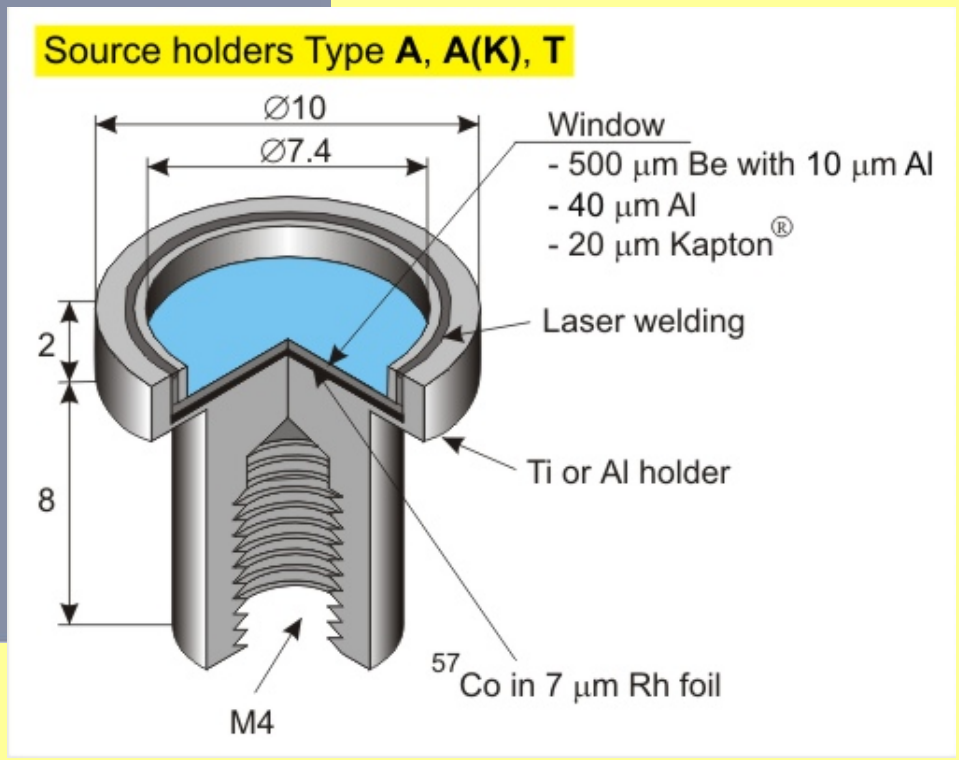



Reference Absorbers

Activity = 10 - 270 mCi, lifetime 10 y

1 Ci = 37 GBq

# $^{119m}$Sn Mössbauer Source

$^{119m}$Sn source = $CaSnO_3$ matrix with $^{119m}$Sn
Activity = 2 - 40 mCi, lifetime 10 y

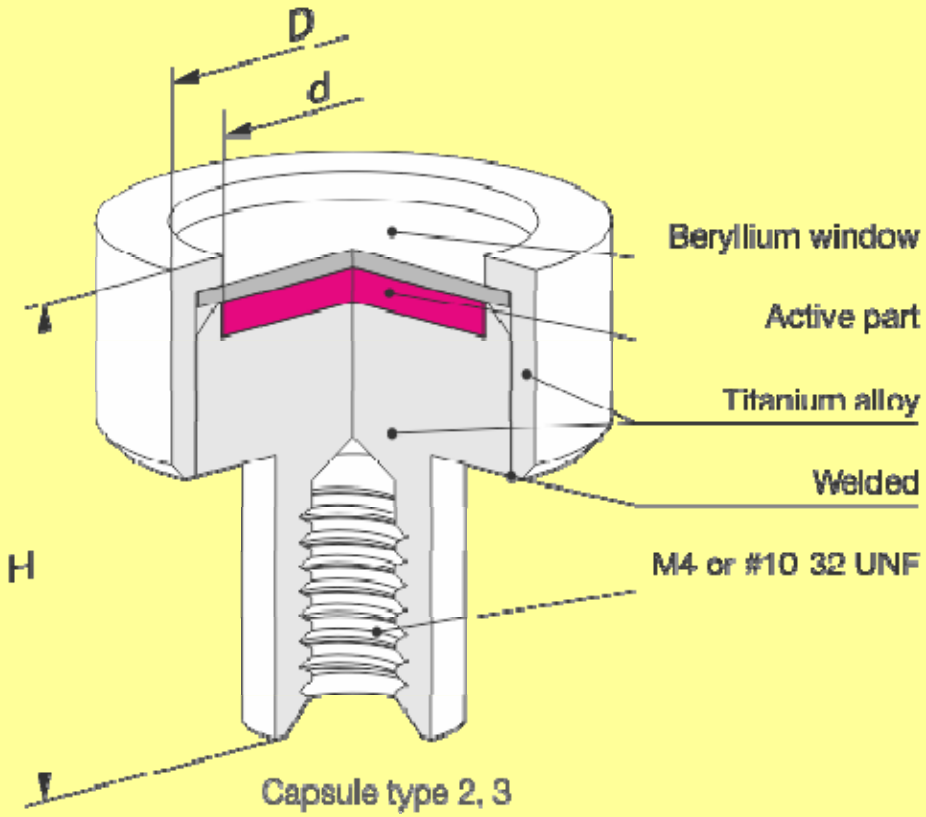


$^{119}$Sn Mössbauer uses the 23.87 keV level which is populated by the decay of 245 day $^{119m}$Sn

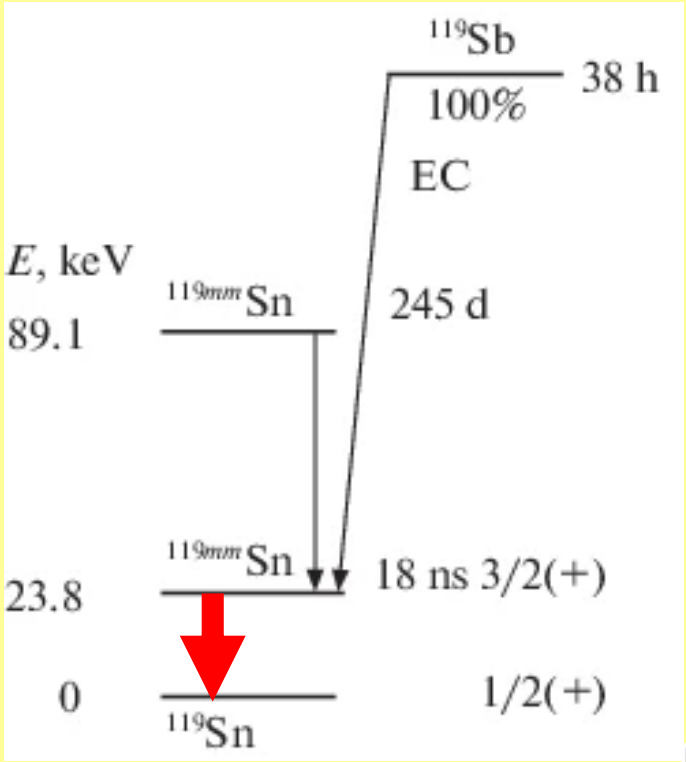

# Mean Lifetime $\tau$ of Excited State and Natural Line Width $\Gamma$

An excited state (nuclear or electronic) of **mean lifetime $\tau$** does not have a sharp energy value, but only a value within the energy range $\Delta E$

The **Heisenberg Uncertainty Principle:**
$\Delta E \, \Delta t \geq \hbar/2$

**Natural line width** $\Gamma = \hbar / \tau$

Transitions from an excited (e) to the ground state (g) involve all energies within the range of $\Delta E$

The transition probability or intensity as a function of E = **a spectral line** centered around the most probable transition energy $E_0$

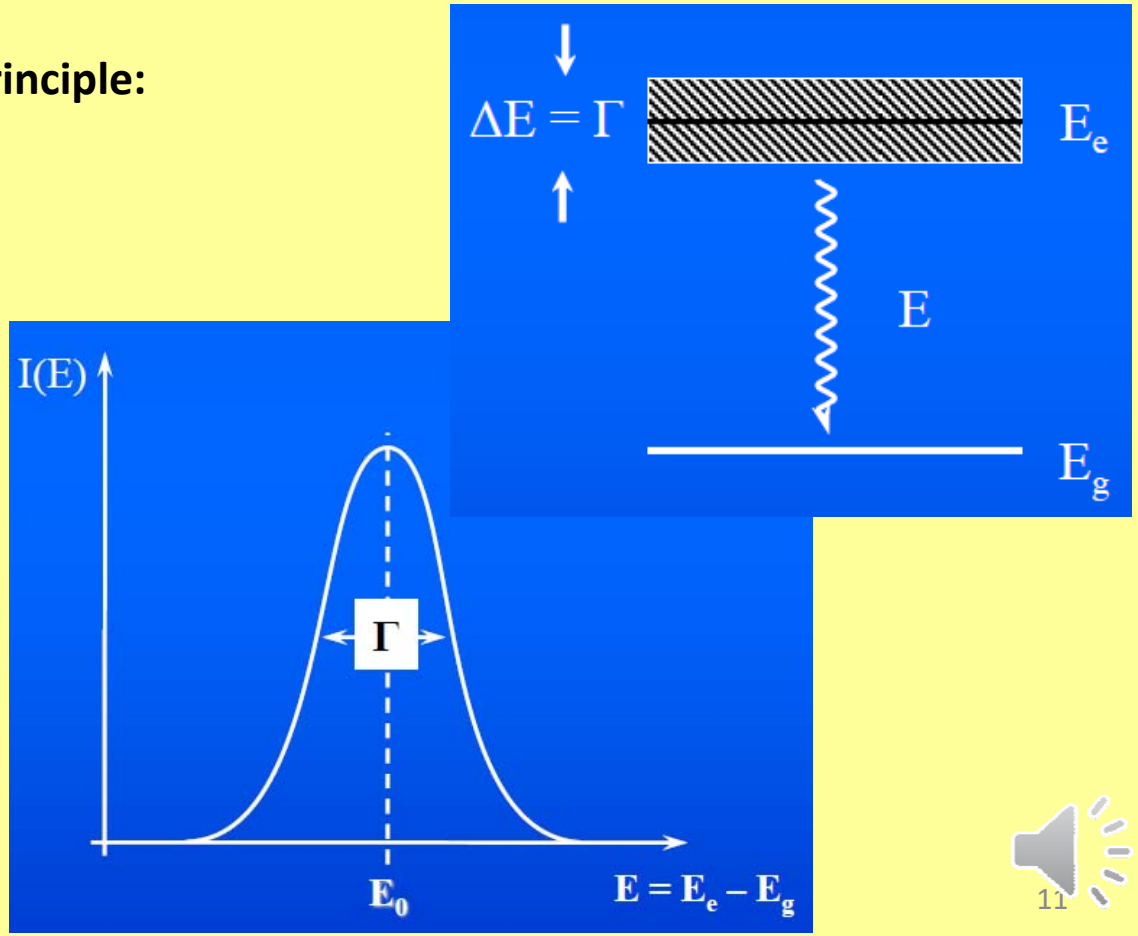

# Transition Probability

**Lorentzian formula for spectral line shape**

$$I(E) = \frac{(\Gamma/2)^2}{(E - E_0)^2 + (\Gamma/2)^2}$$

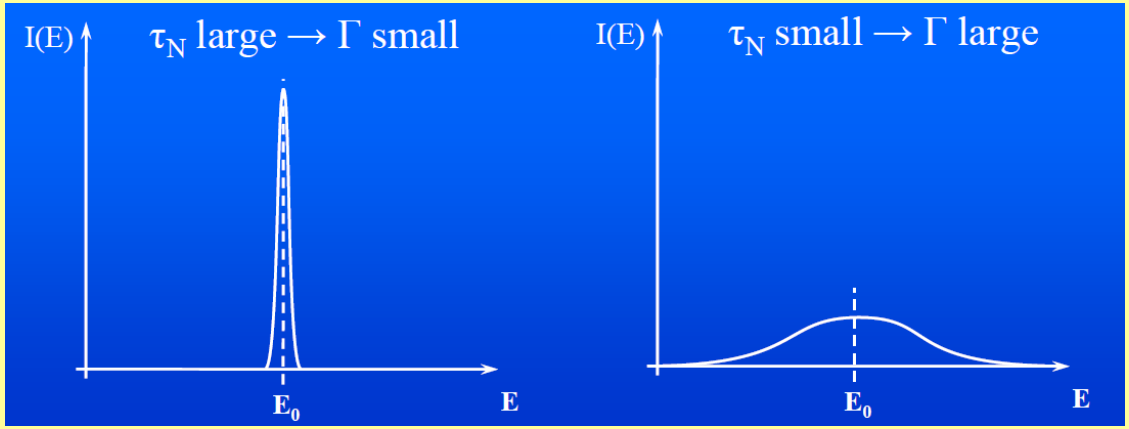


The width at half maximum of the spectral line = **natural line width** $\Gamma$ determined by the mean lifetime $\tau$

$^{57}$Fe (14.4 keV)
$\tau = 1.43\ 10^{-7}$ s = 143 ns
$\Gamma = 4.6\ 10^{-9}$ eV

**Long lifetime = sharp lines**

**Short lifetime = broad lines**

**Resonance** absorption is **observable** only if the emission and absorption lines **overlap sufficiently**
This is not the case when the lines are too narrow or too broad

Suitable for Mössbauer spectroscopy: lifetime = **$10^{-6}$ – $10^{-11}$ s**

# Recoil Effect

$^{57}$Fe (14.4 keV)
$\Gamma$ = 4.6 $10^{-9}$ eV

$$E_R = \frac{E_\gamma^2}{2mc^2}$$

**Recoil energy $E_R = 2 \times 10^{-3}$ eV**

Much larger (5-6 orders of magnitude) than the natural line width
= no resonance possible between free atoms

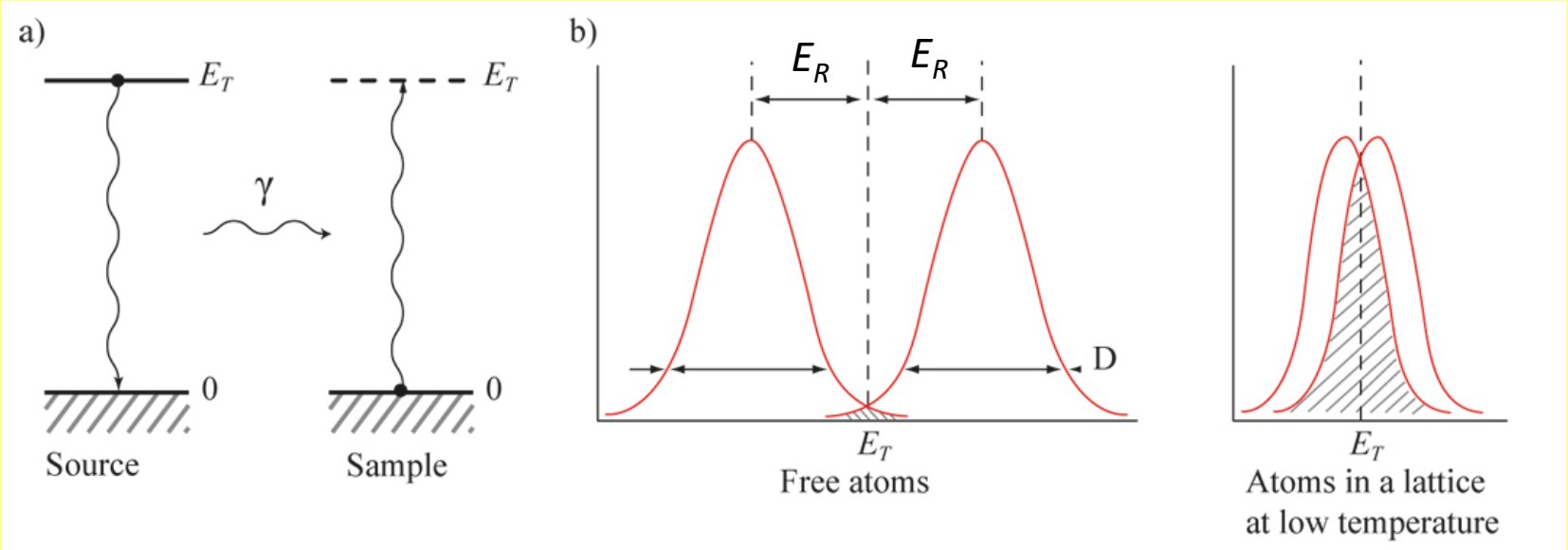


**The Mössbauer effect cannot be observed for freely moving atoms or molecules, i.e. in gaseous or liquid state**

# Recoilless Emission and Absorption

**Solid state**, crystalline or non-crystalline = atoms tightly bound in the lattice
Unshifted transition lines overlap = nuclear resonance absorption **observed**

$$E_R = \frac{E_\gamma^2}{2mc^2}$$

Large mass M of a solid particle as compared to an atom = the linear momentum created by emission and absorption of a gamma quantum practically vanishes

The **recoil** energy is mostly transferred to the lattice **vibrational** system
The vibrational energy of the lattice can only change by discrete amounts 0, $\pm\hbar\omega$, $\pm 2\hbar\omega$, …

The probability that no lattice excitation (zero-phonon processes) takes place during γ-emission or absorption = ***f*** (Debye-Waller or Lamb-Mössbauer factor)

*f* denotes the **fraction** of nuclear transitions which occur **without recoil**
Only for this fraction is the Mössbauer effect observable

# Debye-Waller or Lamb-Mössbauer Factor

$$f = \exp\left[-\frac{E_R}{k_B \Theta_D}\left(\frac{3}{2}+\frac{\pi^2 T^2}{\Theta_D^2}\right)\right]$$

**Recoil-less fraction *f*** increases with:

- decreasing recoil energy $E_R$
- decreasing temperature T
- increasing Debye temperature $\theta_D = h\omega_D/2\pi k_B$

$\omega_D$ = vibrational frequency of Debye oscillator, $k_B$ = Boltzmann factor

$\theta_D$ = a measure for the strength of the bonds between the Mössbauer atom and the lattice

**Stronly bound atoms** = larger $\theta_D$ = **less recoil**

# Mössbauer Experiment

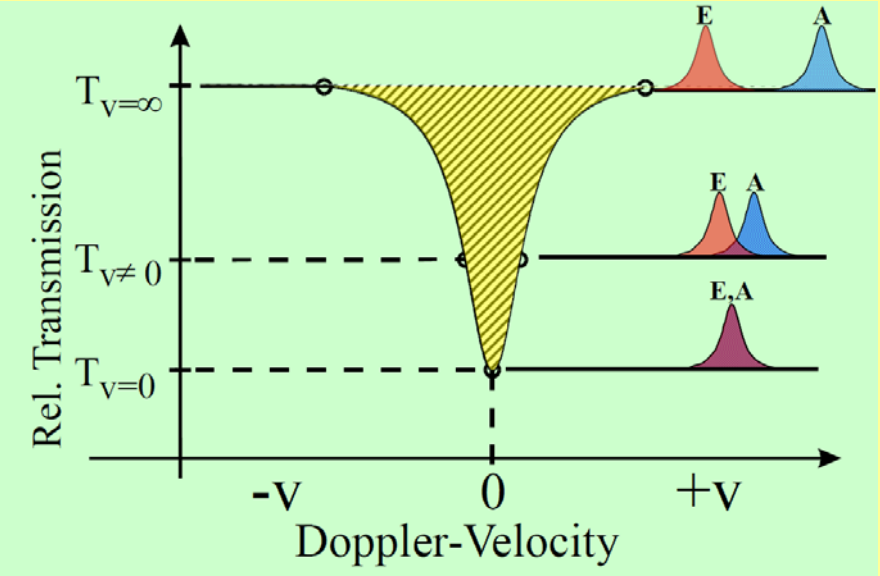


The resonance perturbed by electric and magnetic **hyperfine interactions** between the nuclei and electric and magnetic fields set up by electrons

Hyperfine interactions **shift** and **split** degenerate nuclear levels resulting in several transition lines

The Mössbauer source emits a single transition line E (assume the absorber shows also only one transition line A)

E and A have slightly modified transition energies, perturbation energies $10^{-8}$ eV comparable to the natural linewidth, shifts the transition lines away from each other such that the overlap decreases or disappears entirely

Overlap restored by the **Doppler effect**, i.e. by moving the absorber and the source relative to each other

# Mössbauer Experiment

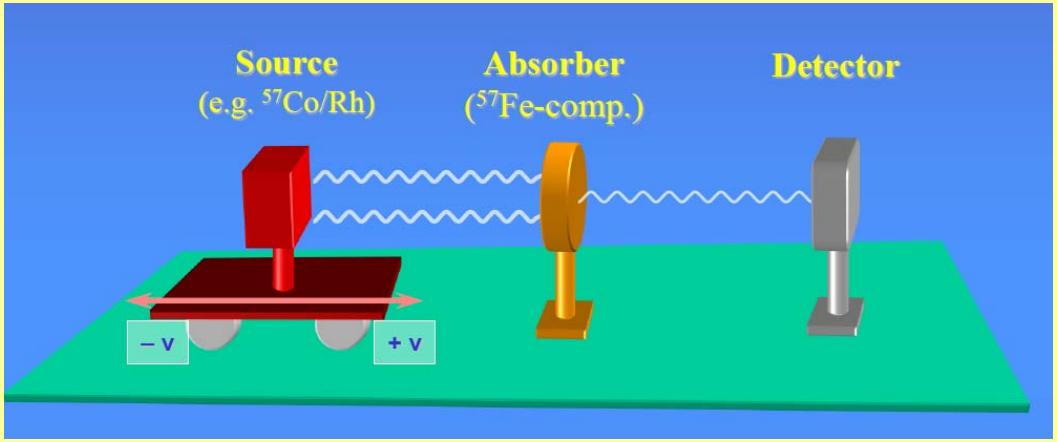


Source and absorber are moved relative to each other

**Doppler velocity**

$$v = c\frac{\Gamma}{E_\gamma}$$

**$^{57}$Fe :** Γ = 4.7 $10^{-9}$ eV, $E_\gamma$ = 14.41 keV, c = speed of light

***v* = 0.096 mm s$^{-1}$**

A velocity of **10 mm s$^{-1}$** provides an energy shift

ΔE = 4.8 × $10^{-7}$ eV

$$\Delta E = \frac{v}{c}E_\gamma$$

# Mössbauer Experiment

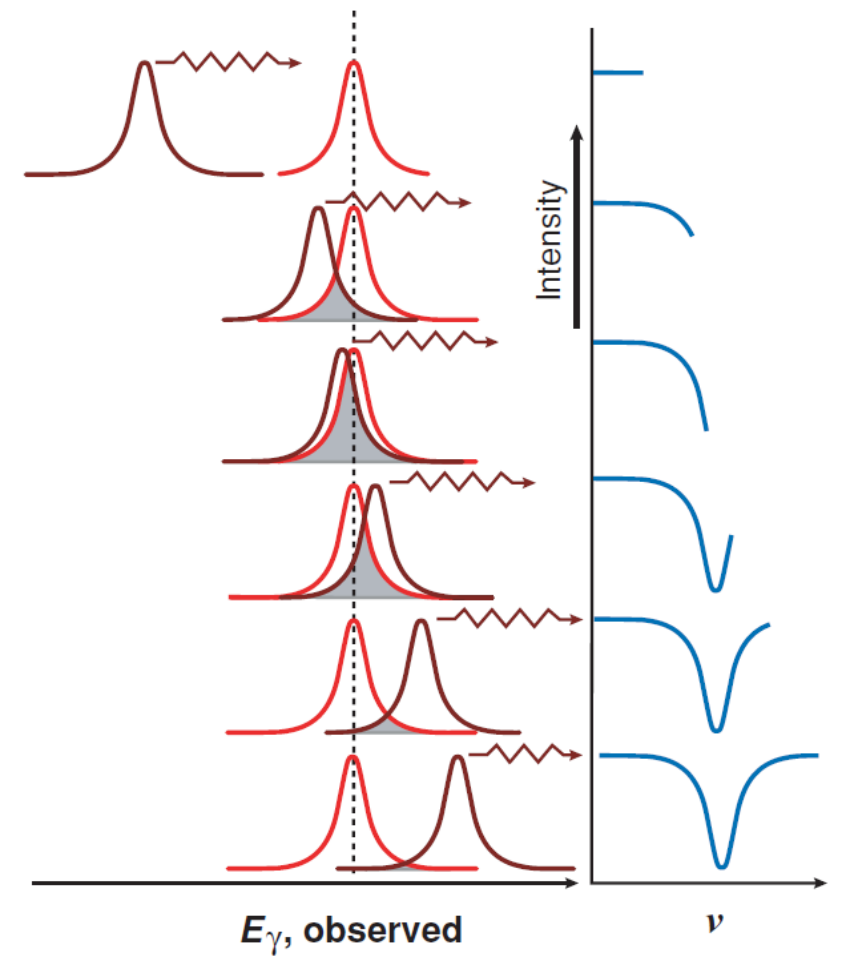


The source is moved at Doppler velocity v
This shifts the center of the emission spectrum (*brown*) from smaller to larger energies, relative to the center of the absorption spectrum (*red* ), whose center, the quantized transition energy, is fixed

The level of **the transmission spectrum** (*blue*) at each value of velocity, *v*, is determined by how much the shifted emission spectrum overlaps the absorption spectrum

A greater overlap results in reduced transmission owing to resonant absorption

The evolution of the transmission spectrum from large negative (source moving away from absorber) to large positive values of velocity is shown from the top to the bottom rows

# Mössbauer Experiment

Controls the electro-mechanical vibrator

4.2 K b.p. of liquid He
1.5 K by pumping on the liquid He vessel

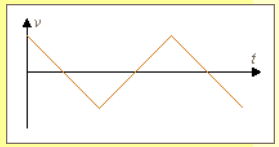

Constant acceleration

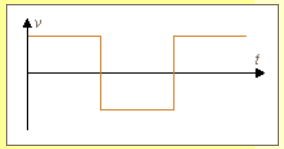

Constant velocity

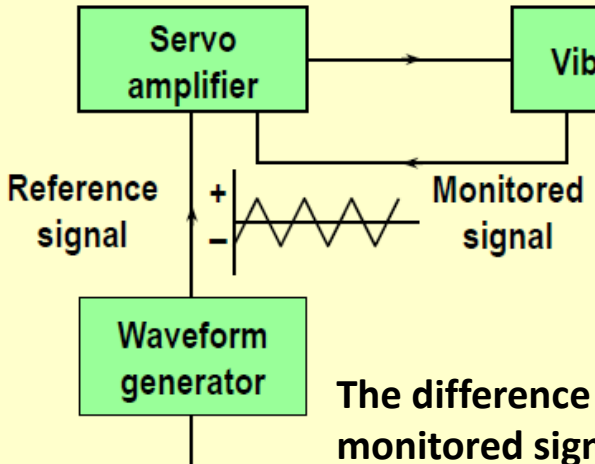


Transmission intensity

The difference between the monitored signal and the reference signal drives the vibrator at the same frequency (typically 50 Hz)

Non-resonant background radiation rejected

Synchronises a triangular voltage waveform yielding a linear Doppler velocity scale as the channel address advances

Data output (display, magnetic tape, etc.)

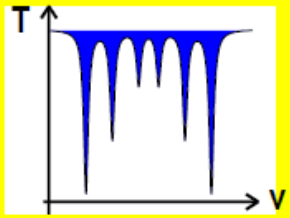


Several hundred channels synchronised with the vibrator

# Correlation of Count Rate with Channel Number and Relative Velocity

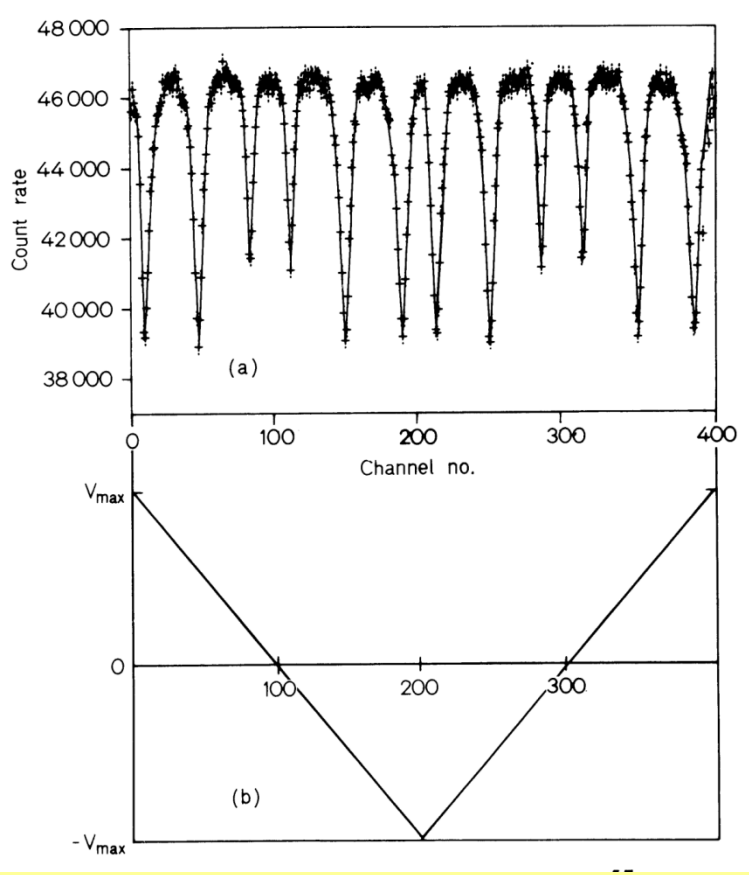


**Mössbauer spectrum** of metallic Fe

The count rate is plotted as function of the channel number

Doppler velocity as a function of the channel number

# Hyperfine Interactions between Nuclei and Electrons

## Mössbauer Parameters = Chemical infomation from electrons

**oxidation state, coordination, spin state HS/LS, magnetic ordering, ligands…**

—Electric Monopole Interaction = **Isomer Shift** $\delta$

—Electric Quadrupole Interaction = **Quadrupole Splitting** $\Delta E_Q$

—Magnetic Dipole Interaction = **Magnetic Splitting** $\Delta E_M$

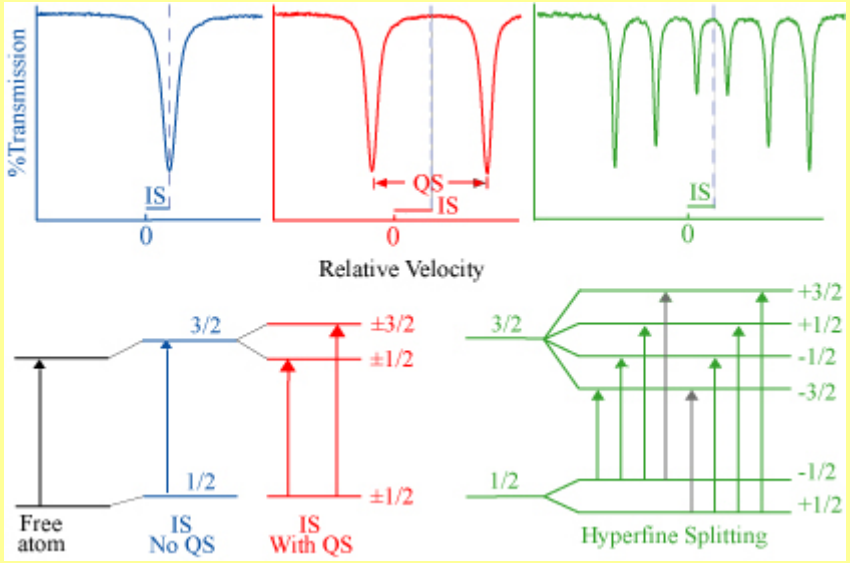


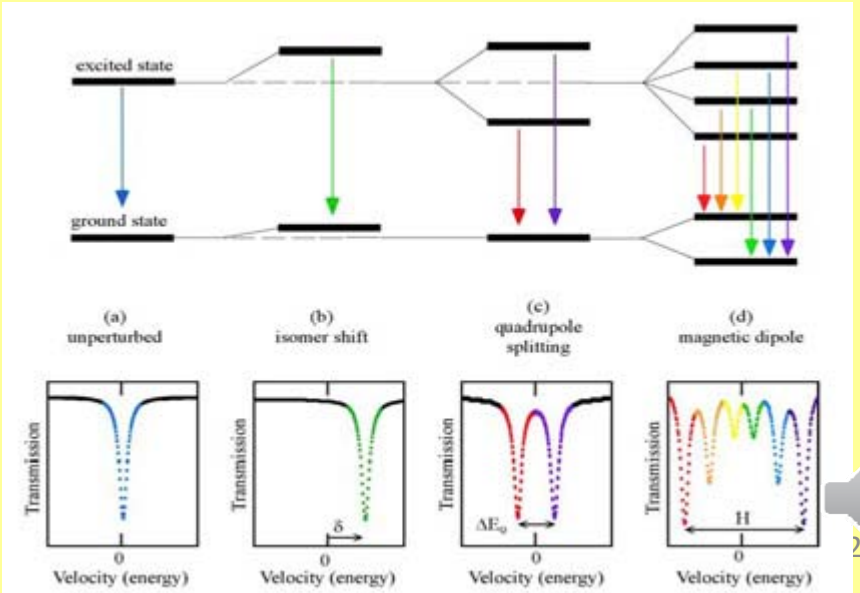

# Hyperfine Interactions

**Electric monopole interaction (Coulombic)**
between protons of the nucleus and **s-electrons** penetrating the nuclear field
**Different shifts** of nuclear levels E and A
Isomer shift values give information on the oxidation state, spin state, and bonding properties, such as covalency and electronegativity

**Electric quadrupole interaction**
between the nuclear **quadrupole** moment ($eQ \neq 0$, $I > ½$) and an inhomogeneous electric field at the nucleus ($EFG \neq 0$)
Nuclear states split into $I + ½$ substates
The quadrupole splitting gives the information on oxidation and spin state, site symmetry

**Magnetic dipole interaction**
between the nuclear magnetic dipole moment ($\mu \neq 0$, $I > 0$) and a **magnetic field** ($H \neq 0$) at the nucleus
Nuclear states split into $2I + 1$ substates with $m_I = +I, +I - 1, ...., -I$
The magnetic splitting gives information on the magnetic properties of the material under study - ferromagnetism, antiferromagnetism

# Isomer Shift $\delta$

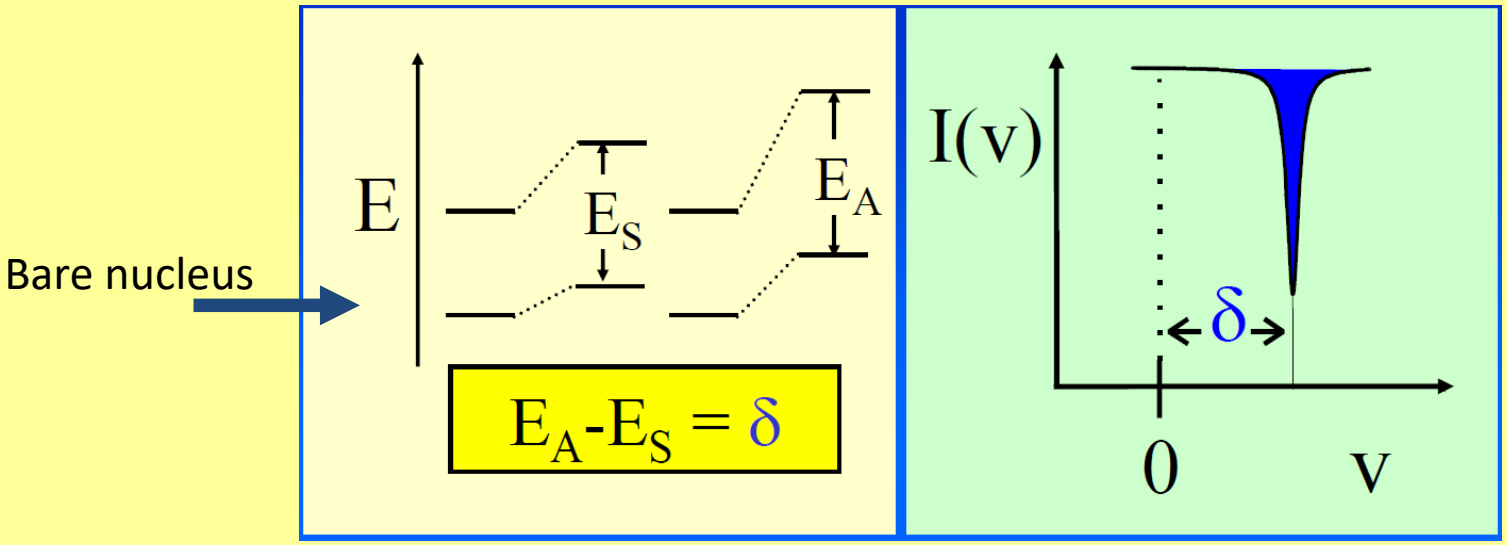


**The nuclear radius** in the **excited** state is **different** (in $^{57}$Fe smaller) than that in the **ground** state: $\mathbf{R_e \neq R_g}$

The electronic **densities** of all *s*-electrons (1s, 2s, 3s, etc.) are different at the nuclei of the source and the absorber: $\mathbf{\rho_S \neq \rho_A}$ $\quad \rho = |\psi(0)|^2$

The result is that **the electric monopole interactions** (Coulomb interactions) are different in the source and the absorber and therefore affect the nuclear ground and excited state levels to a different extent - this leads to the measured **isomer shift *δ***

# Isomer Shift $\delta$

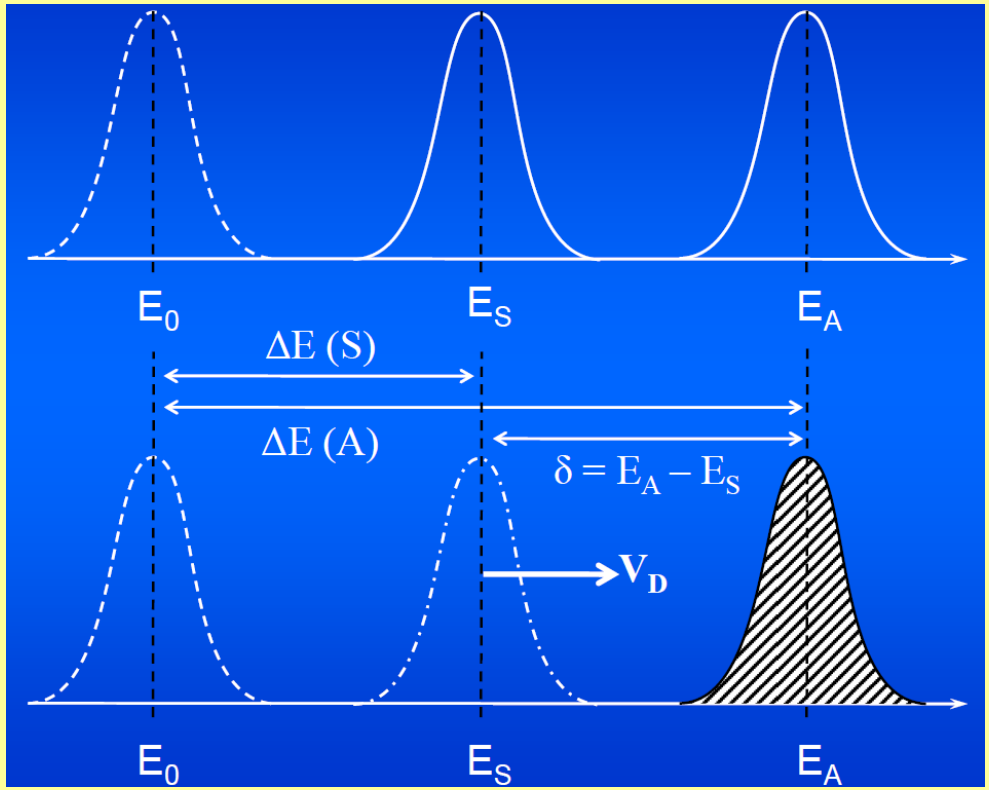


$\delta = E_A - E_S = C\,(\rho_A - \rho_S)(R_e^2 - R_g^2)$

$C = (2/3)\pi Z e^2$

$\rho = |\psi(0)|^2$

The energy levels of the ground and excited states of **a bare nucleus $E_0$** are perturbed and shifted by electric monopole interactions - Coulombic interactions

The shifts in the ground and excited states differ = **different nuclear radii** and **different electron densities** in the source and absorber material

The individual energy differences $E_S$ and $E_A$ cannot be measured

A Mössbauer experiment measures only the difference of the transition energies $\delta = E_A - E_S$, **isomer shift**

# Isomer Shift $\delta$

The isomer shift depends **directly** on the ***s*-electron** densities and is influenced **indirectly** via shielding by ***p*-, *d*-, and *f*-electrons** which are not capable of penetrating the nuclear field

$$\delta = C\,\{|\Psi(0)|_A^2 - |\Psi(0)|_S^2\}(R_e^2 - R_g^2)$$

$C = (2/3)\pi Ze^2$

**Influence on the *s*-electron densities at the nucleus $|\Psi(0)|^2$ (r = 0)**

**Direct** = change of electron **population in *s*-orbitals** (mainly valence *s*-orbitals) changes directly $|\Psi(0)|^2$

**Indirect** = **shielding by *p*-, *d*-, *f*-electrons**, increase of electron density in *p*-, *d*-, *f*-orbitals increases shielding effect for *s*-electrons from the nuclear charge
→ *s*-electron cloud expands, $|\Psi(0)|^2$ at nucleus decreases

# Isomer Shift $\delta$

$$\delta = C\,\{|\Psi(0)|_A^2 - |\Psi(0)|_S^2\}(R_e^2 - R_g^2)$$

The more **electronegative** the ligands the lower the **electron density** of the **nucleus under observation (A)** and consequently the isomer shift changes

The direction of change depends on the quantity $(R_e^2 - R_g^2)$
The difference of nuclear radii in the excited and ground state
The change in the mean-square radius of the nucleus

$(R_e^2 - R_g^2) < 0$ the isomer shift increases with increasing ligand electronegativity

$(R_e^2 - R_g^2) > 0$ the isomer shift decreases with increasing ligand electronegativity

# Isomer Shift in $^{119}$Sn Mössbauer Spectra

$$\delta = C\,\{|\Psi(0)|_A^2 - |\Psi(0)|_S^2\}(R_e^2 - R_g^2)$$

$(R_e^2 - R_g^2) > 0$

$+3.3\ 10^{-3}$ fm$^2$

The nuclear radius in the **excited** state is **larger** than that in the **ground** state

| Compound | $\delta$/ mm s$^{-1}$ | Compound | $\delta$/ mm s$^{-1}$ |
|---|---|---|---|
| $SnF_4$ | –0.36 | Sn (gray) | 2.02 |
| $SnO_2$ | 0.0 | Sn (white) | 2.50 |
| $SnCl_4$ | 0.85 | SnO | 2.71 |
| $SnBr_4$ | 1.15 | $SnSO_4$ | 3.90 |
| $SnI_4$ | 1.55 | $SnF_2$ | 3.2 |
| $SnPh_4$ | 1.22 | $SnCl_2$ | 4.07 |
| $SnH_4$ | 1.27 | $SnBr_2$ | 3.93 |

$Sn^0$

$5s^2\ 5p^2$

Sn(IV) $\delta <$ 2.00 mm s$^{-1}$ electron config. $5s^0\ 5p^0$ – lower el. density at nucleus than neutral $Sn^0$ atom = negative shift

Sn(II) $\delta >$ 2.50 mm s$^{-1}$ electron config. $5s^2\ 5p^0$ – higher el. density at nucleus than neutral Sn atom as no 5p shielding = positive shift

# Isomer Shift in $^{119}$Sn Mössbauer Spectra

$(R_e^2 - R_g^2) > 0$

$$\delta = C\,\{|\Psi(0)|_A^2 - |\Psi(0)|_S^2\}(R_e^2 - R_g^2)$$

Sn (white)
$\delta$ = 2.50 mm s$^{-1}$

Sn (gray)
$\delta$ = 2.02 mm s$^{-1}$

**$SnO_2$**
**$\delta$ = 0 mm s$^{-1}$**

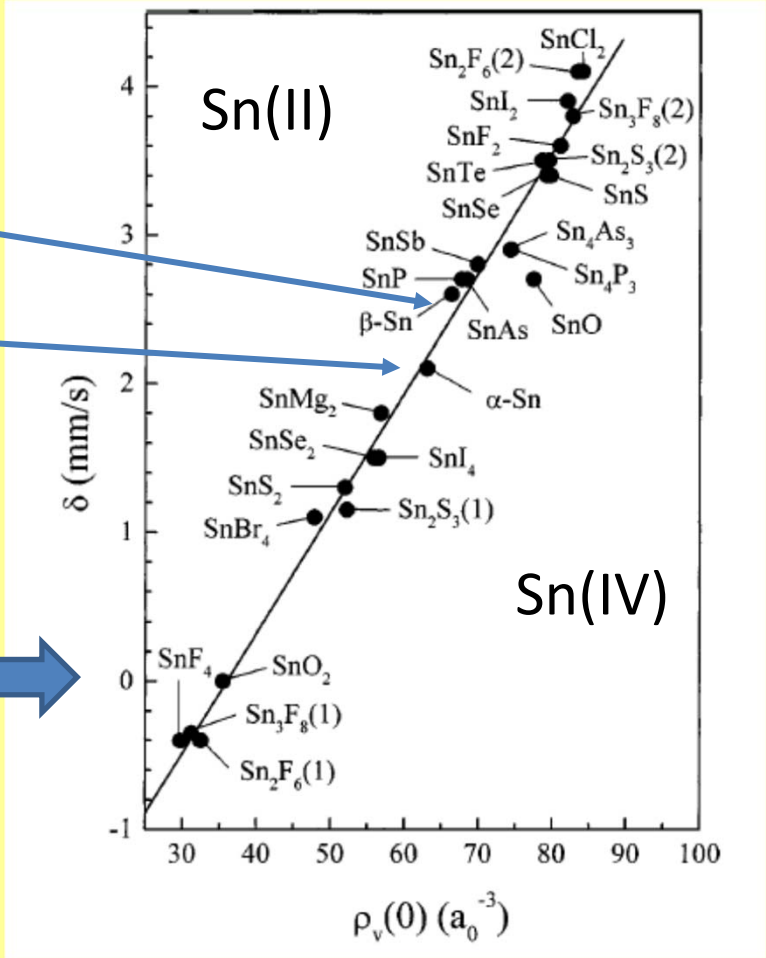


The isomer shift decreases with decreasing value of the valence electron density at the nucleus $\rho_v(0)$

# Isomer Shift in $^{119}$Sn Mössbauer Spectra

$(R_e^2 - R_g^2) > 0$

$$\delta = C\{|\Psi(0)|_A^2 - |\Psi(0)|_S^2\}(R_e^2 - R_g^2)$$

**Sn (gray)**

**$\delta$ = 0 mm s$^{-1}$**

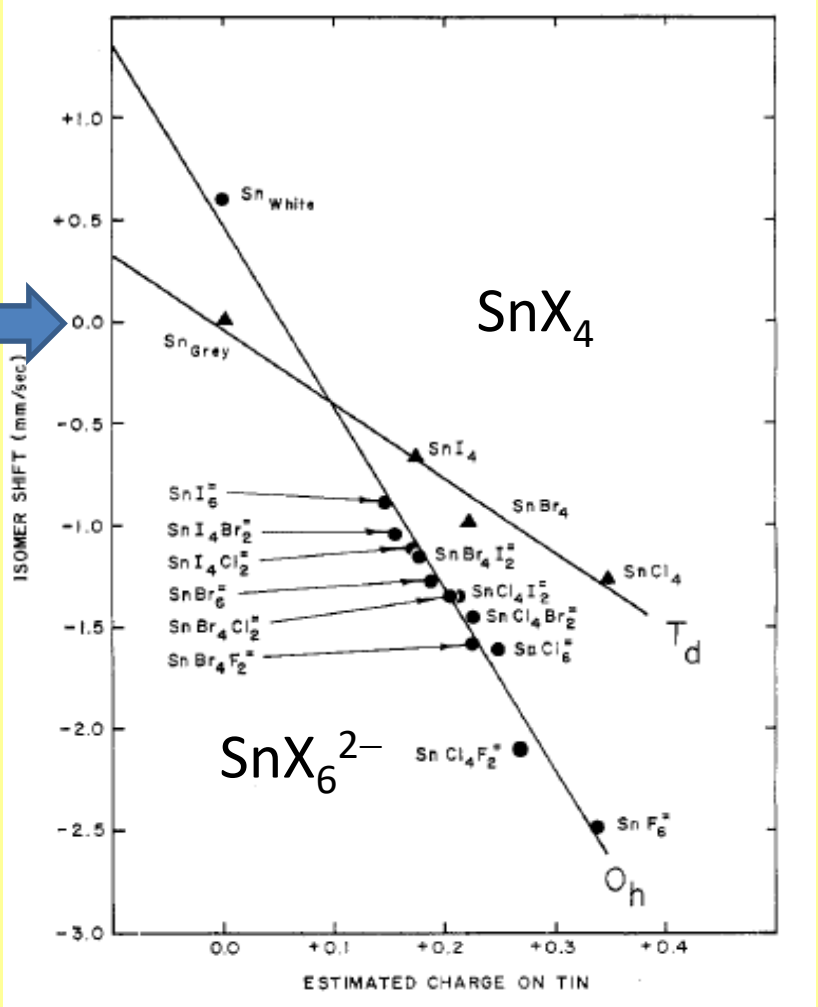


Sn(IV)

The isomer shift decreases with increasing ligand electronegativity and increasing positive charge at the Sn nucleus

# Isomer Shift in $^{119}$Sn Mössbauer Spectra

$(R_e^2 - R_g^2) > 0$

$$\delta = C\{|\Psi(0)|_A^2 - |\Psi(0)|_S^2\}(R_e^2 - R_g^2)$$

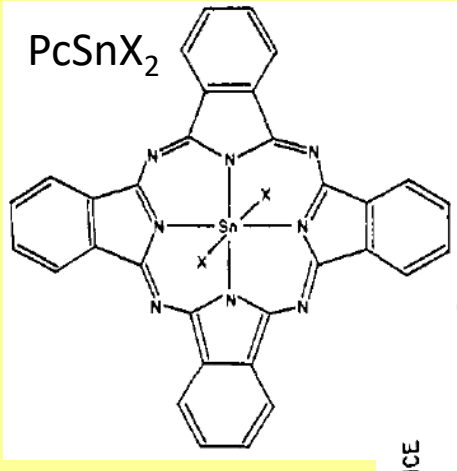


Dihalophthalocyaninotin(IV)
X = F, OH, Cl, Br, I

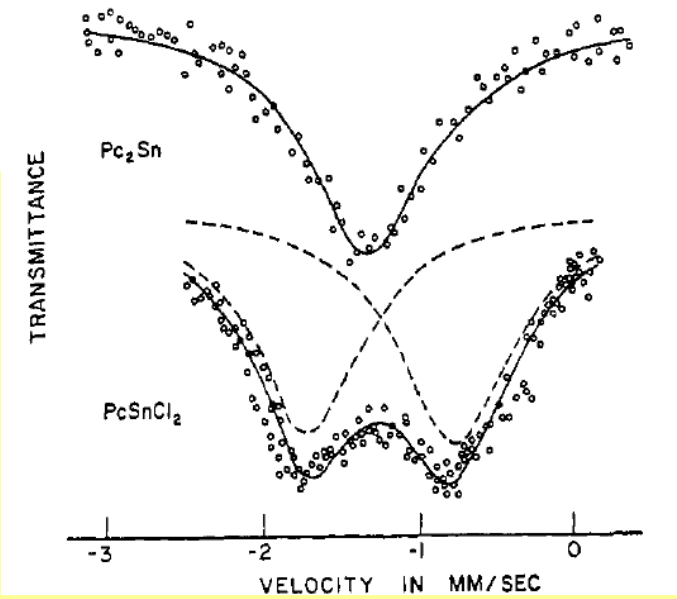


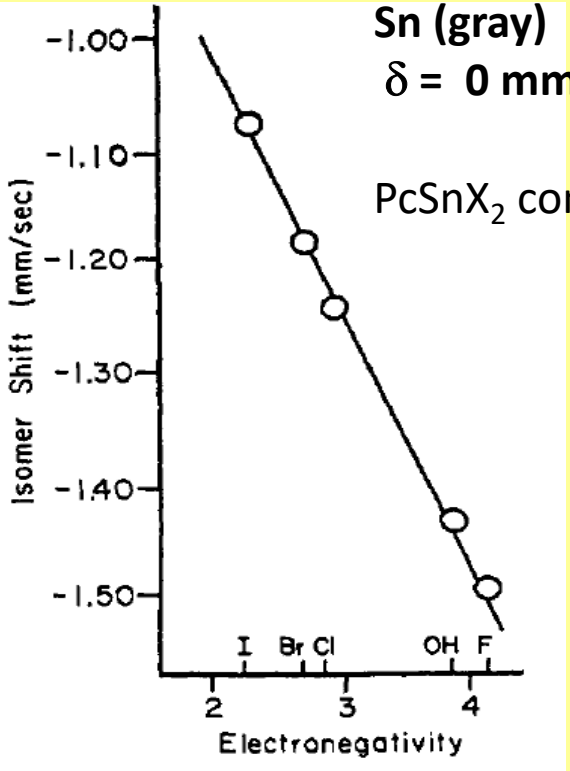


**Sn (gray)**
**$\delta$ = 0 mm s$^{-1}$**

$PcSnX_2$ complexes

The isomer shift decreases with increasing ligand electronegativity

# Isomer Shift in $^{119}$Sn Mössbauer Spectra

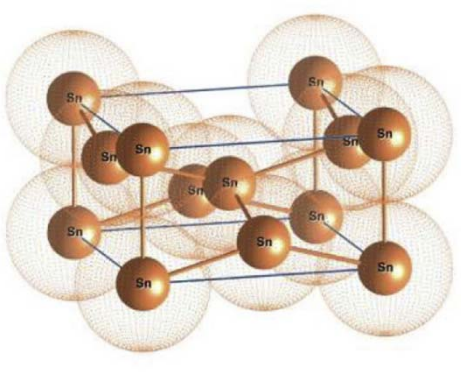

A large difference between Moessbauer-Lamb factors at room temperature increases the sensitivity of gray-Sn (0.16) over white-Sn (0.04)

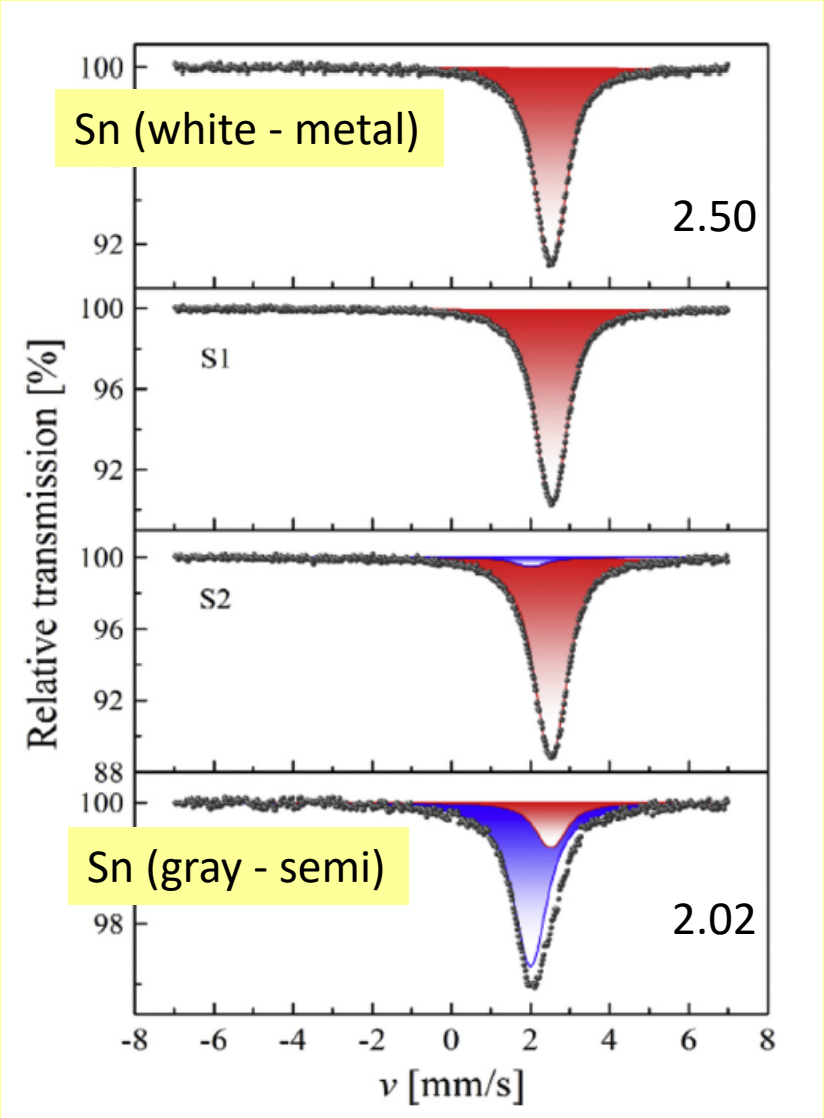


**white → gray** transition in Sn

A large volume expansion (26.3%)

Coordination 6(4+2) → 4

Reduced s-electron densities at Sn - the lower electron density corresponds to smaller value of isomer shift

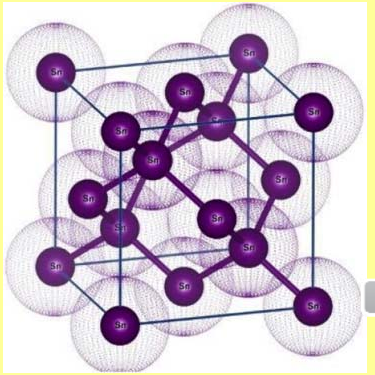

Materials Chemistry and Physics 182 (2016) 10

# Electron Densities at the $^{57}Fe$ Nucleus

| Electrons per cubic Bohr radius | $3d^8$ | $3d^7$ $Fe^+$ | $3d^6$ $Fe^{2+}$ | $3d^5$ $Fe^{3+}$ | $3d^64s^2$ free atom |
|---|---|---|---|---|---|
| $\lvert\psi_{1s}(0)\rvert^2$ | 5378.005 | 5377.973 | 5377.840 | 5377.625 | 5377.873 |
| $\lvert\psi_{2s}(0)\rvert^2$ | 493.953 | 493.873 | 493.796 | 493.793 | 493.968 |
| $\lvert\psi_{3s}(0)\rvert^2$ | 67.524 | 67.764 | 68.274 | 69.433 | 68.028 |
| $\lvert\psi_{4s}(0)\rvert^2$ | | | | | 3.042 |
| $2\sum_n \lvert\psi_{ns}(0)\rvert^2$ | 11878.9 | 11879.2 | 11879.8 | 11881.7 | 11885.8 |

*s*-electron density increases


[1] Watson, R. E. (1960) *Phys. Rev.*, **118**, 1036.
[2] Watson, R. E. (1960) *Phys. Rev.*, **119**, 1934.


The partial electron densities refer to one electron each in 1s, 2s, 3s, 4s-orbitals

The total *s*-electron density at r = 0 is twice the sum of the partial one-electron contributions (all *s*-orbitals are doubly occupied)

# Isomer Shifts $\delta$ of Fe Compounds

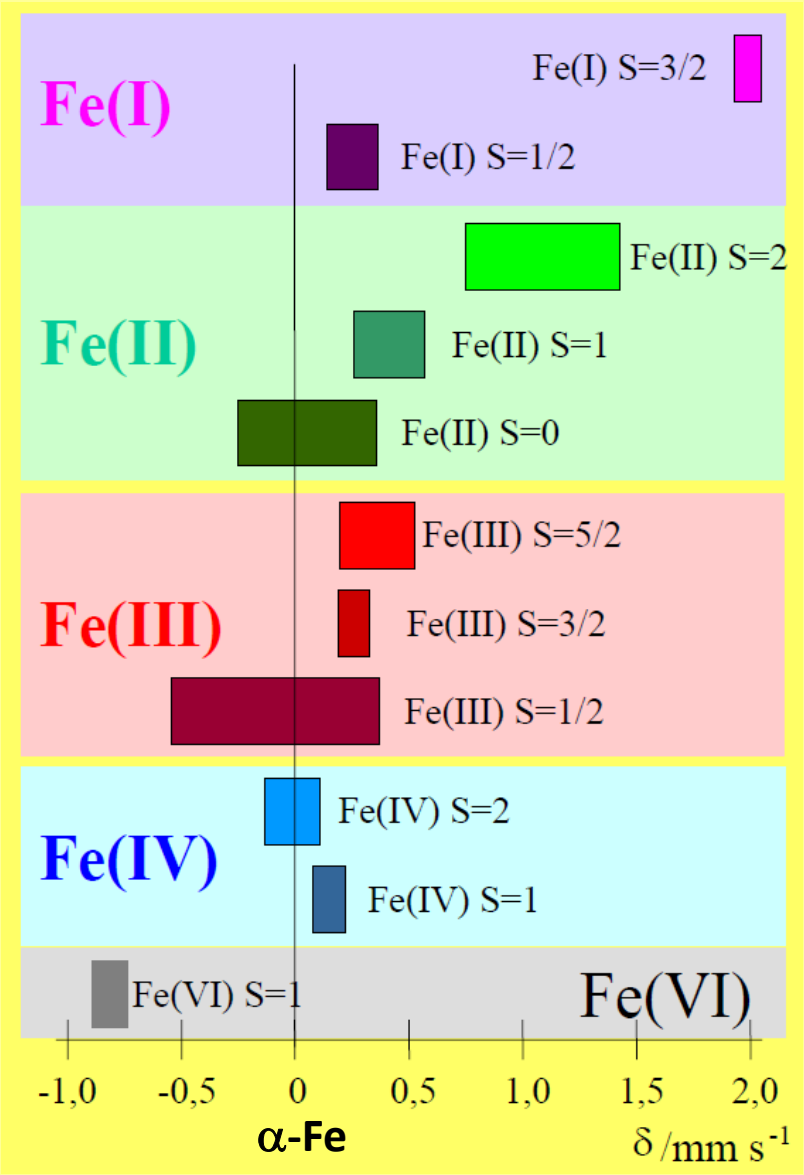


The most positive isomer shift occurs for **Fe(I)** with spin S = 3/2
The seven d-electrons exert a very strong shielding of the s-electrons, this reduces the s-electron density $\rho_A$ giving a strongly negative quantity $(\rho_A - \rho_S)$, as $(R_e^2 - R_g^2) < 0$ for $^{57}Fe$, the isomer shift becomes strongly positive

**Fe(II)** HS with S = 2 can be easily assigned

**Fe(II)**, **Fe(III)**, **Fe(IV)** - overlapping δ values - ambiguous assignment, need to consider the quadrupole splitting parameter

Strongly negative for **Fe(VI)** with spin S = 1
There are only two d-electrons, the shielding effect for s-electrons is very weak and the s-electron density $\rho_A$ at the nucleus becomes high

# Effect of Ligand Electronegativity

$$\delta = C\,\{|\Psi(0)|_A^2 - |\Psi(0)|_S^2\}(R_e^2 - R_g^2)$$

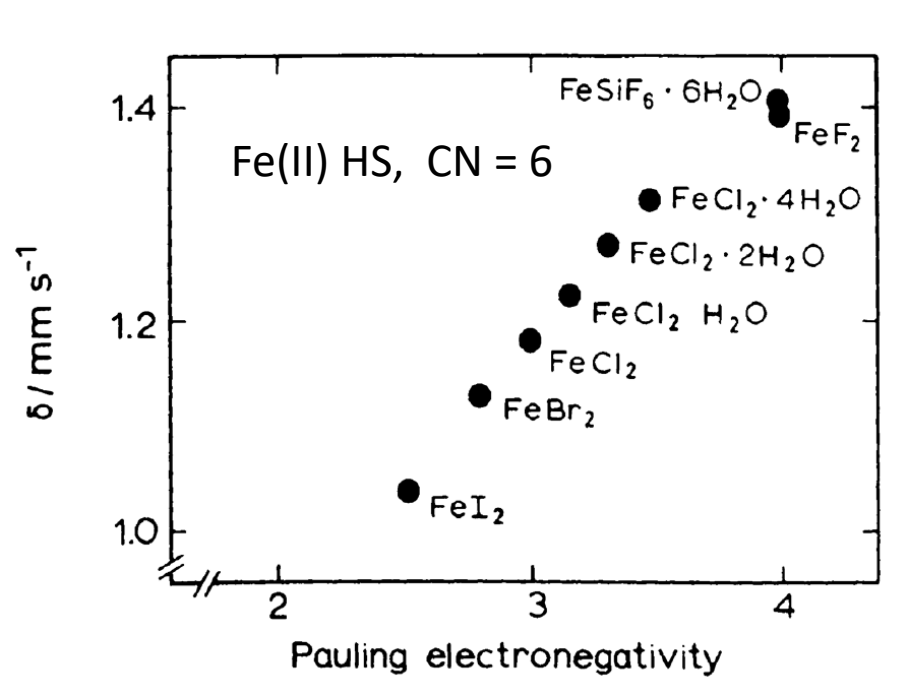


The electronegativity increases from I to F

In the same ordering the s-electron density at the iron nucleus $\rho_A$ decreases

Making $(\rho_A - \rho_S)$ more negative

$(R_e^2 - R_g^2) < 0$ for $^{57}Fe$

The isomer shift increases from iodide to fluoride

# Second-Order Doppler Shift

**The isomer shifts δ**, i.e., the resonance peak shifts observed in Mössbauer spectra, are composed of two terms:

$$\delta = \delta_C + \delta_{SOD}(T)$$

The first term is the ***chemical isomer shift*** $\delta_C$ which is temperature-independent

The second term is the ***second-order Doppler shift*** $\delta_{SOD}$
Since $\delta_{SOD}$ is T-dependent, the observed isomer shift δ is also T-dependent

The **second-order Doppler shift** $\delta_{SOD}$ is related to the mean-square velocity $\langle v^2 \rangle$ of lattice vibrations in the direction of the γ-ray propagation, which increases with increasing T
Accordingly, the Mössbauer resonance moves to a more negative velocity with increasing T :

$$\delta_{SOD} = -\frac{\langle v^2 \rangle}{2c}$$

# Electric Quadrupole Interaction

**Quadrupole Splitting $\Delta E_Q$** **$^{57}$Fe**

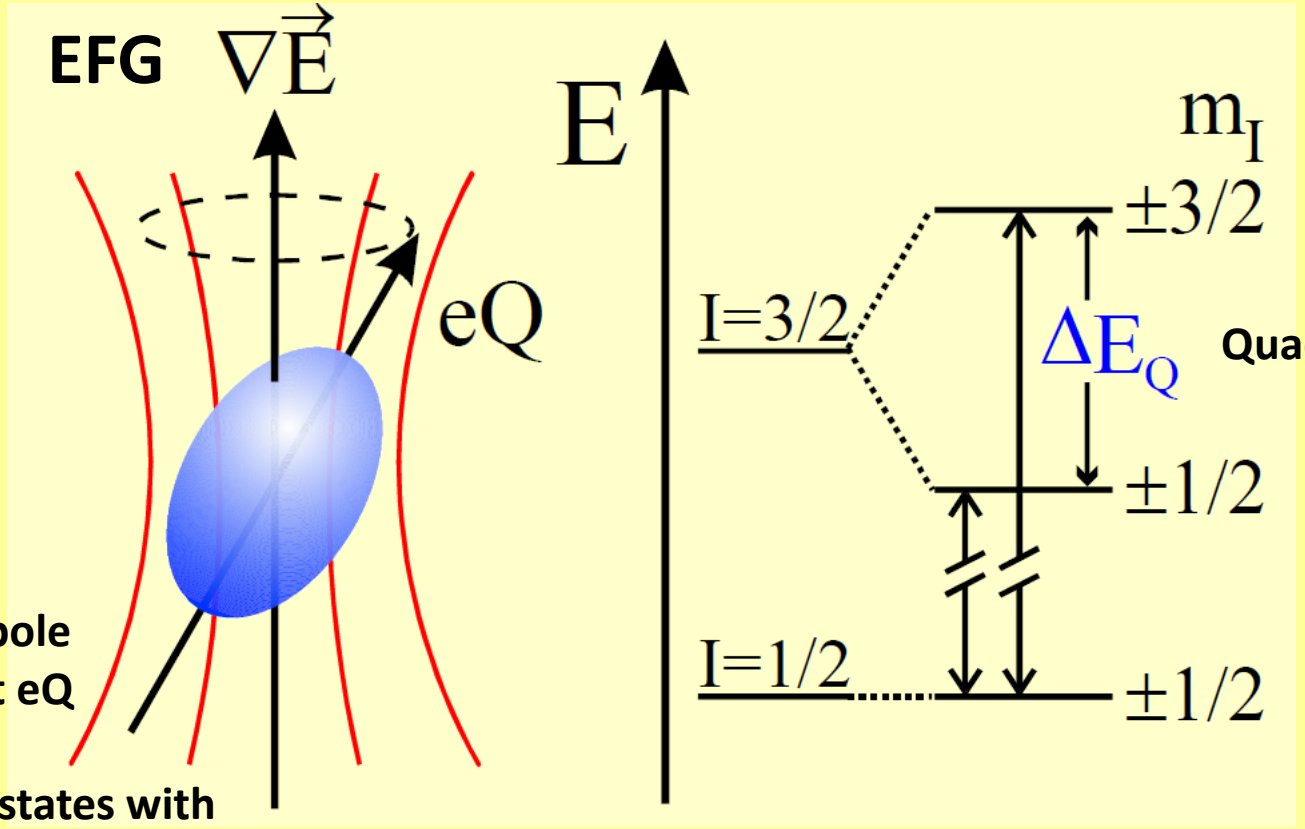


**Quadrupole Moment eQ**

**Nuclear states with *I* > 1/2**

Nuclear states split into ***I* + ½** substates

# Electric Quadrupole Interaction

Electric quadrupole interaction occurs if **at least one of the nuclear states** involved possesses **a quadrupole moment** eQ (for $I > 1/2$) and if **the electric field** at the nucleus is **inhomogeneous (electric field gradient EFG)**

$^{57}$**Fe**: the first excited state (14.4 keV) has a **spin $I$ = 3/2** and therefore also an electric quadrupole moment eQ

EFG is zero in cubic symmetry
EFG is non-zero in:

- non-cubic **valence electron distribution**
- non-cubic **lattice site symmetry**

The precession of the quadrupole moment vector about the field gradient axis

Quadrupole Splitting $\Delta E_Q$ of the degenerate $I$ = 3/2 level into 2 substates with **magnetic spin quantum numbers $m_I$** = ±3/2 and ±1/2

**Selection rule: $\Delta m_I = 0, \pm 1$**

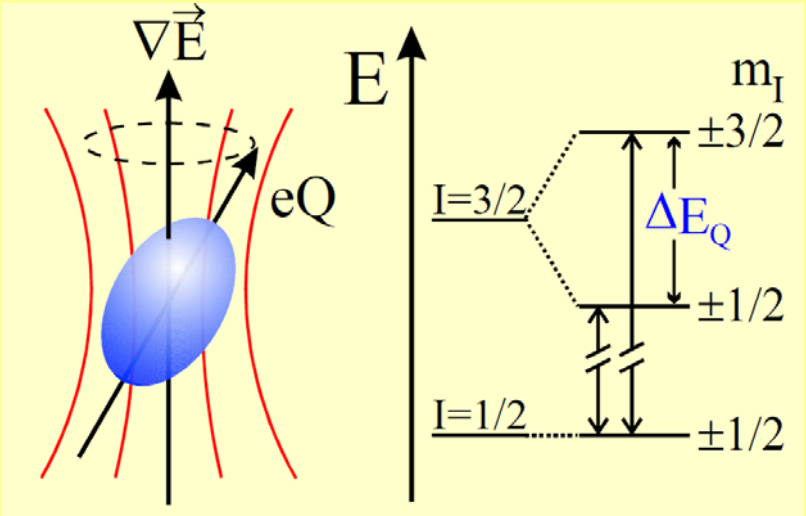


The ground state $I$ = ½

- no quadrupole moment
- unsplit ($I$ + ½ = 1)
- twofold degenerate

# Electric Quadrupole Interaction

Quadrupole Splitting $\Delta E_Q$

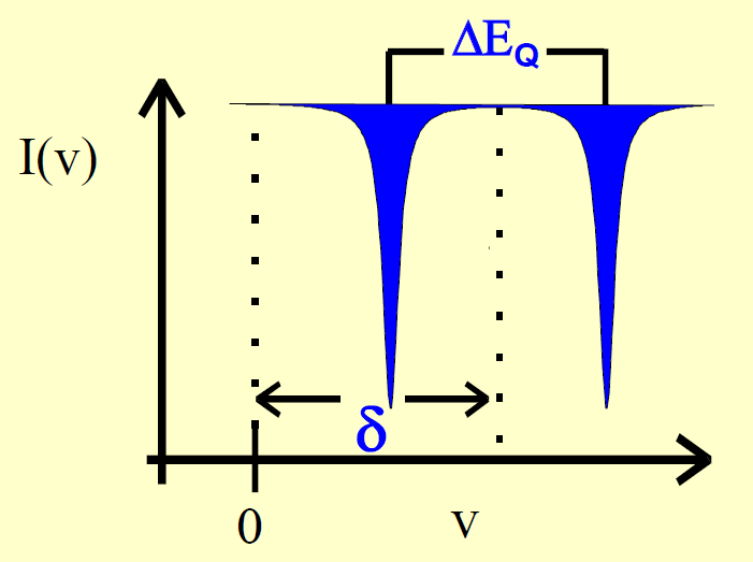


**Selection rule: $\Delta m_I = 0, \pm 1$**

**$^{57}$Fe - 2 transitions allowed**

The energy difference between the two substates $\Delta E_Q$ is observed in the spectrum as the separation between the two resonance lines

$$E_Q(I, m_I) = \frac{eQV_{zz}}{4I(2I-1)}\left[3m_I^2 - I(I+1)\right]\left(1+\frac{\eta^2}{3}\right)^{\frac{1}{2}}$$

$V_{zz}$ component of EFG

$\eta$ - asymmetry parameter

# Electric Quadrupole Interaction

Quadrupole Splitting $\Delta E_Q$

**Selection rule: $\Delta m_I = 0, \pm 1$**

Nuclear states split into ***I* + ½** substates

**$^{57}$Fe** **$^{129}$I** **$^{73}$Ge**

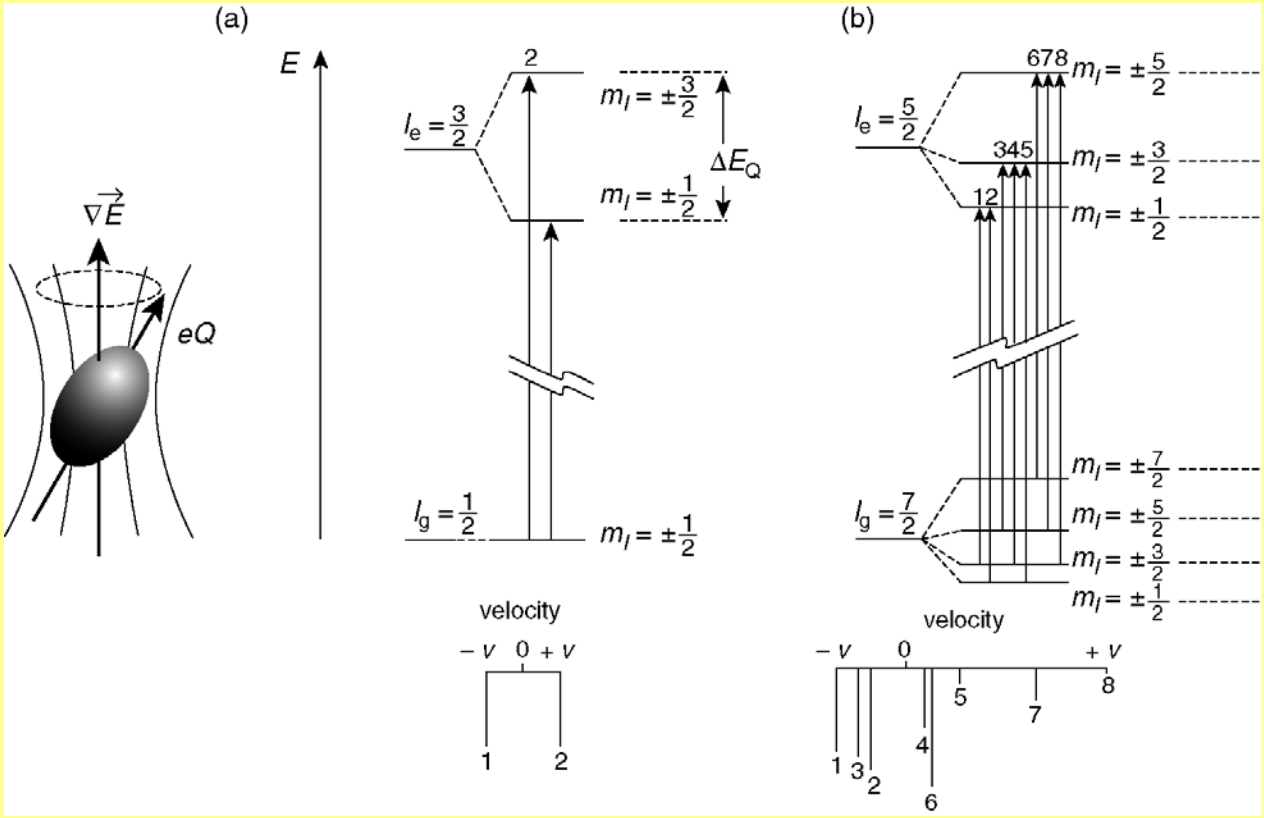


**$I_e$ = 7/2 → 4 levels**

**$I_g$ = 9/2 → 5 levels**

**? lines**

# Electric Field Gradient (EFG)

A point charge $q$ at a distance $r = (x^2 + y^2 + z^2)^{½}$ from the nucleus causes a potential $V(r) = q/r$ at the nucleus

The electric field $E$ at the nucleus is the negative gradient of the potential, $-\nabla V$, and the electric field gradient EFG is given by:

$$EFG = \vec{\nabla}\vec{E} = -\vec{\nabla}\vec{\nabla}V = \begin{vmatrix} V_{xx} & V_{xy} & V_{xz} \\ V_{yx} & V_{yy} & V_{yz} \\ V_{zx} & V_{zy} & V_{zz} \end{vmatrix}$$

$V_{ij} = (\partial^2 V/\partial_i \partial_j)$ (i, j, k = x, y, z)

3 x 3 second rank EFG tensor

Only five $V_{ij}$ components are independent, because:

- symmetric form of the tensor, i.e., $V_{ij} = V_{ji}$,
- Laplace: traceless tensor

$$\sum_i V_{ii} = 0, \quad i = x, y, z$$

**Principal axes system**: $|V_{zz}| \geq |V_{xx}| \geq |V_{yy}|$

- Non-axial symmetry – the asymmetry parameter η: $0 \leq \eta \leq 1$

$$\eta = (V_{xx} - V_{yy})/V_{zz}$$

- Axial symmetry (tetragonal, trigonal) - the EFG is given only by the tensor component $V_{zz}$ , $V_{xx} = V_{yy} \rightarrow \eta = 0$

# Electric Field Gradient (EFG)

Two parameters required to describe **Quadrupole Interaction:** $V_{zz}$ + η

Two kinds of contributions to the EFG: $(EFG)_{total} = (EFG)_{val} + (EFG)_{lat}$
or in the principal axes system and η = 0: $(V_{zz})_{total} = (V_{zz})_{val} + (V_{zz})_{lat}$

- The **lattice contribution** $(V_{zz})_{lat}$ = non-cubic arrangement of the next nearest neighbors

- The **valence contribution** $(V_{zz})_{val}$ = anisotropic (noncubic) electron population in the orbitals

Energy levels

$$E_Q(I, m_I) = \frac{eQV_{zz}}{4I(2I-1)}\left[3m_I^2 - I(I+1)\left(1+\frac{\eta^2}{3}\right)^{\frac{1}{2}}\right]$$

# Electric Field Gradient (EFG)

**For $^{57}$Fe with $I_e = 3/2$, $I_g = 1/2$**
in axially symmetric systems, η = 0

$$E_Q(I, m_I) = \frac{eQV_{zz}}{4I(2I-1)}\left[3m_I^2 - I(I+1)\right]\left(1+\frac{\eta^2}{3}\right)^{\frac{1}{2}}$$

**Energy levels $E_Q(I, m_I)$**

$E_Q\ (3/2, \pm 3/2) = eQV_{zz}/4$ for $I = 3/2$, $m_I = \pm 3/2$

$E_Q\ (3/2, \pm 1/2) = -eQV_{zz}/4$ for $I = 3/2$, $m_I = \pm 1/2$

**The quadrupole splitting energy $\Delta E_Q$**

$\Delta E_Q = E_Q(3/2, \pm 3/2) - E_Q\ (3/2, \pm 1/2) = eQV_{zz}/2$

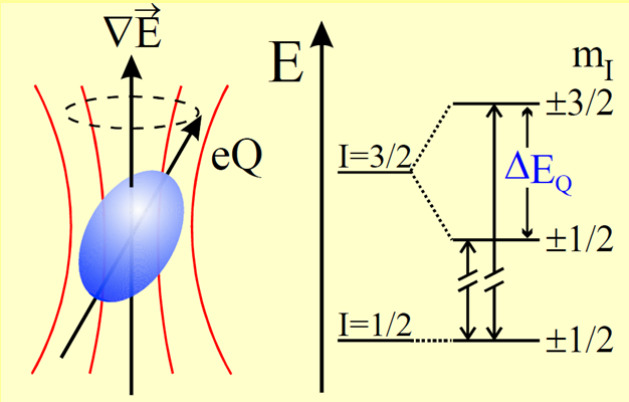

# $[Fe(H_2O)_6](ClO_4)_3$

## $[Fe(H_2O)_6]^{3+}$ Fe(III)-HS, S = 5/2

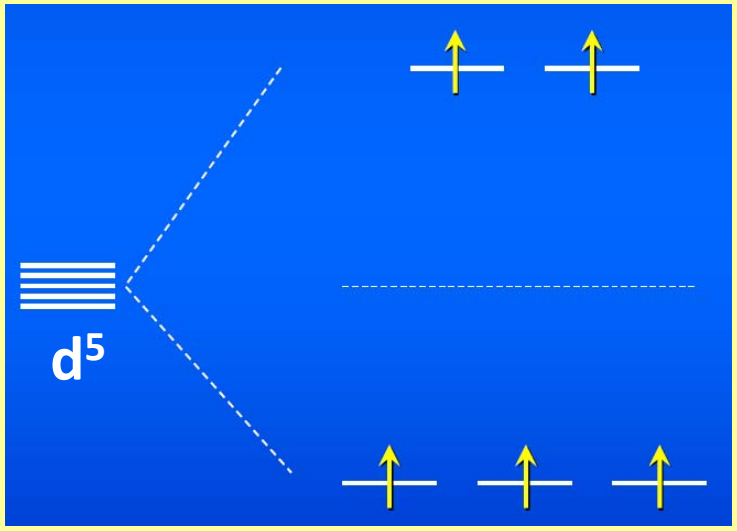


$[ML_6]$ $(O_h)$ $EFG_{lat} = 0$

$^6A_1$ $EFG_{val} = 0$

**Very small quadrupole splitting, below linewidth**

## $^{57}$Fe Mössbauer Spectrum

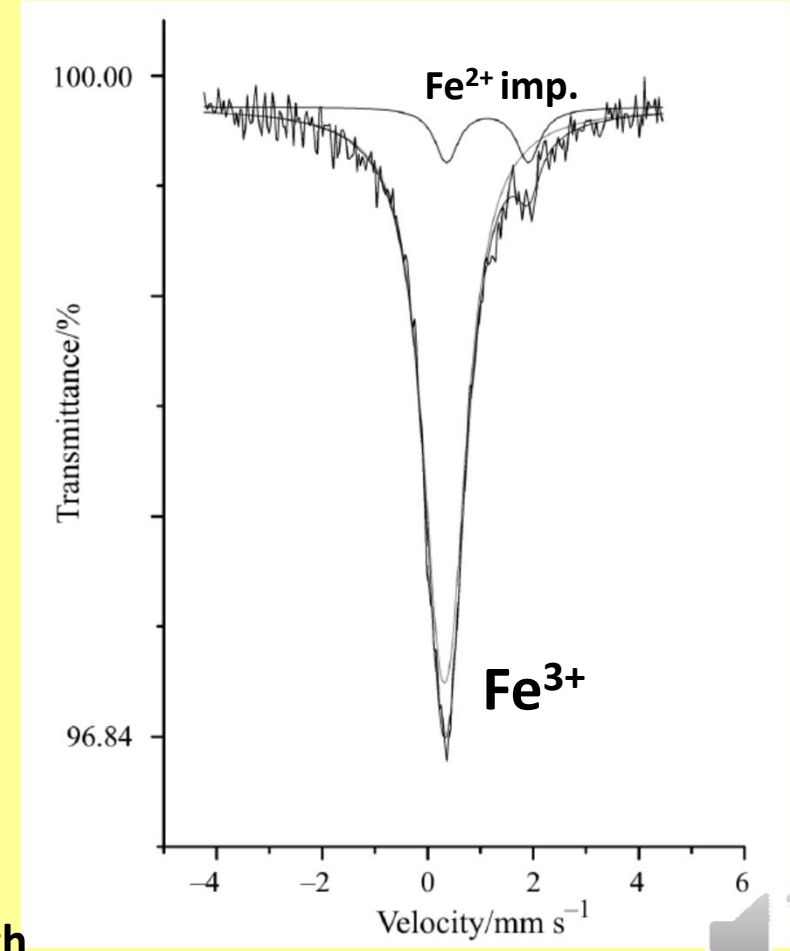

# $FeSO_4 \bullet 7H_2O$

## $[Fe(H_2O)_6]^{2+}$ Fe(II)-HS, S = 2

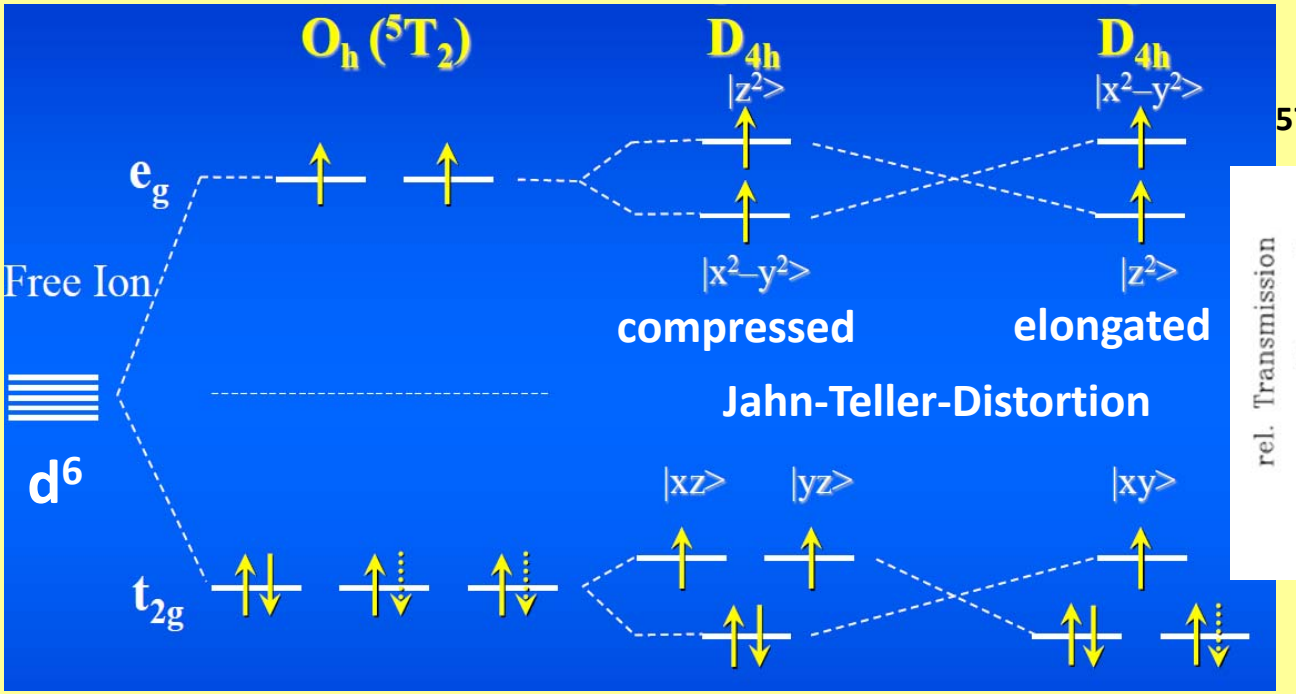


**$^{57}$Fe Mössbauer Spectrum**

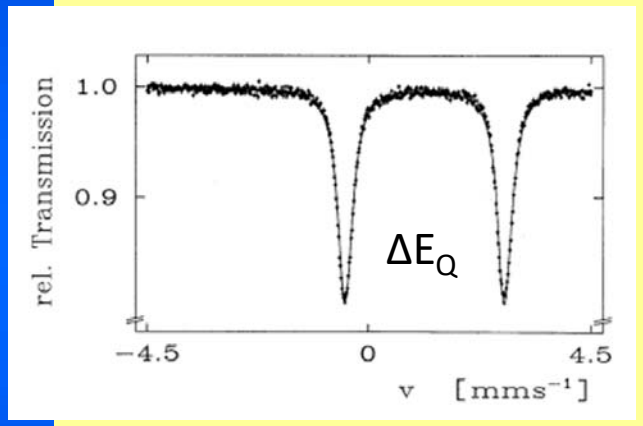


**Quadrupole splitting**

| | | |
|---|---|---|
| $EFG_{lat}$ | = 0 | ≠ 0 |
| $EFG_{val}$ | ≠ 0 | ≠ 0 |

# $K_4[Fe(CN)_6]$

## Fe(II)-LS, S = 0 cubic

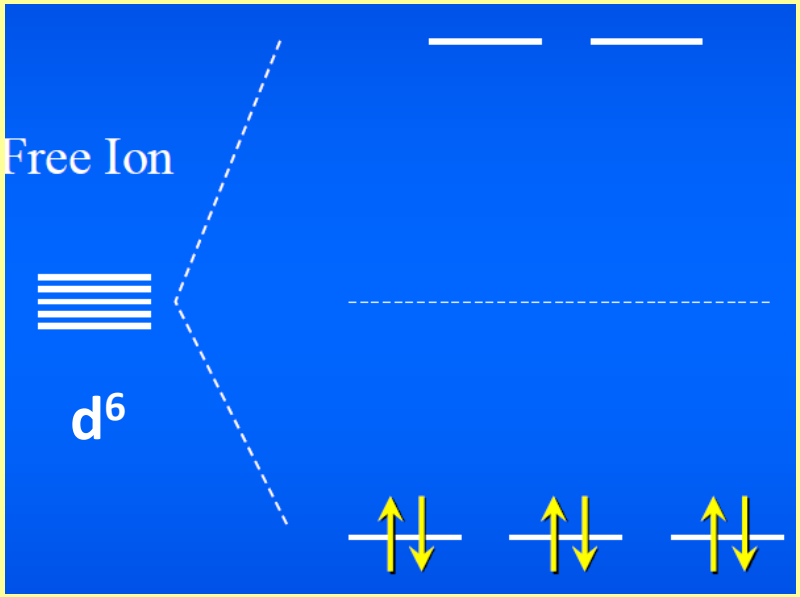


$^{57}$Fe Mössbauer Spectrum

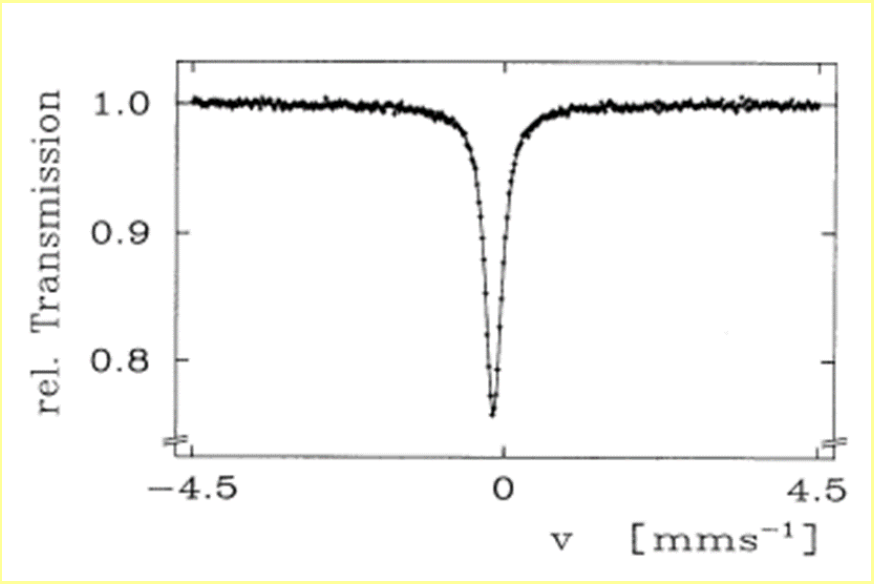


No quadrupole splitting

$[ML_6]$ $(O_h)$ $EFG_{lat} = 0$ $EFG_{val} = 0$

# $Na_2[Fe(CN)_5(NO)]$

**Nitroprusside**

## Fe(II)-LS, S = 0 tetragonal

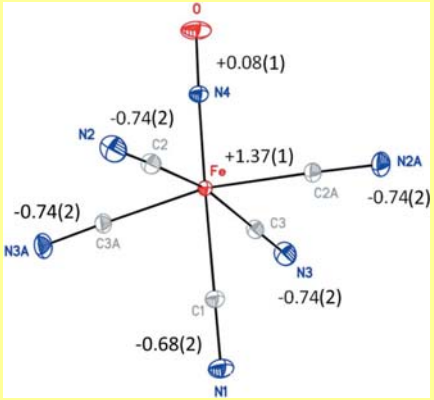


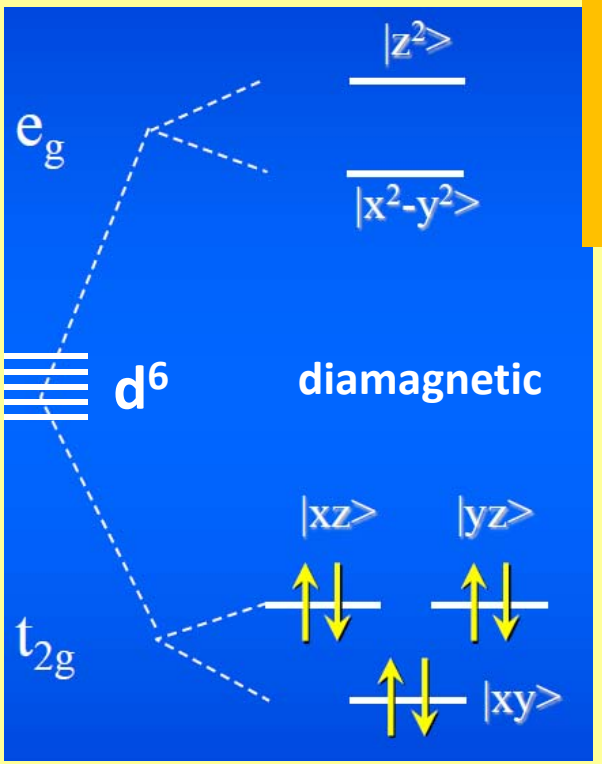


Fe(II) + $NO^+$
or
Fe(III) + NO
or
Fe(IV) + $NO^-$

**$^{57}$Fe Mössbauer Spectrum**

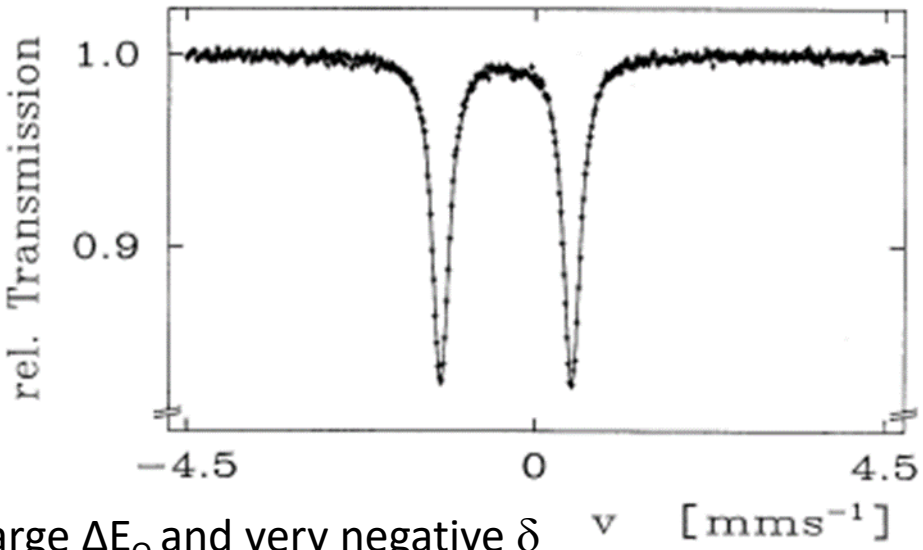


$EFG_{lat} \neq 0$

$EFG_{val} \neq 0$

Unusually large $\Delta E_Q$ and very negative $\delta$ for Fe(II) LS (–0.165 mm/s)
More like Fe(IV)
NO withdraws electron density from $d_{xz}$ and $d_{yz}$ ($\pi$-bonding dp) to its antibonding $\pi$-orbitals

# $^{57}$Fe Mössbauer Spectra Interpretation

## Isomer Shifts and Quadrupole Splitting

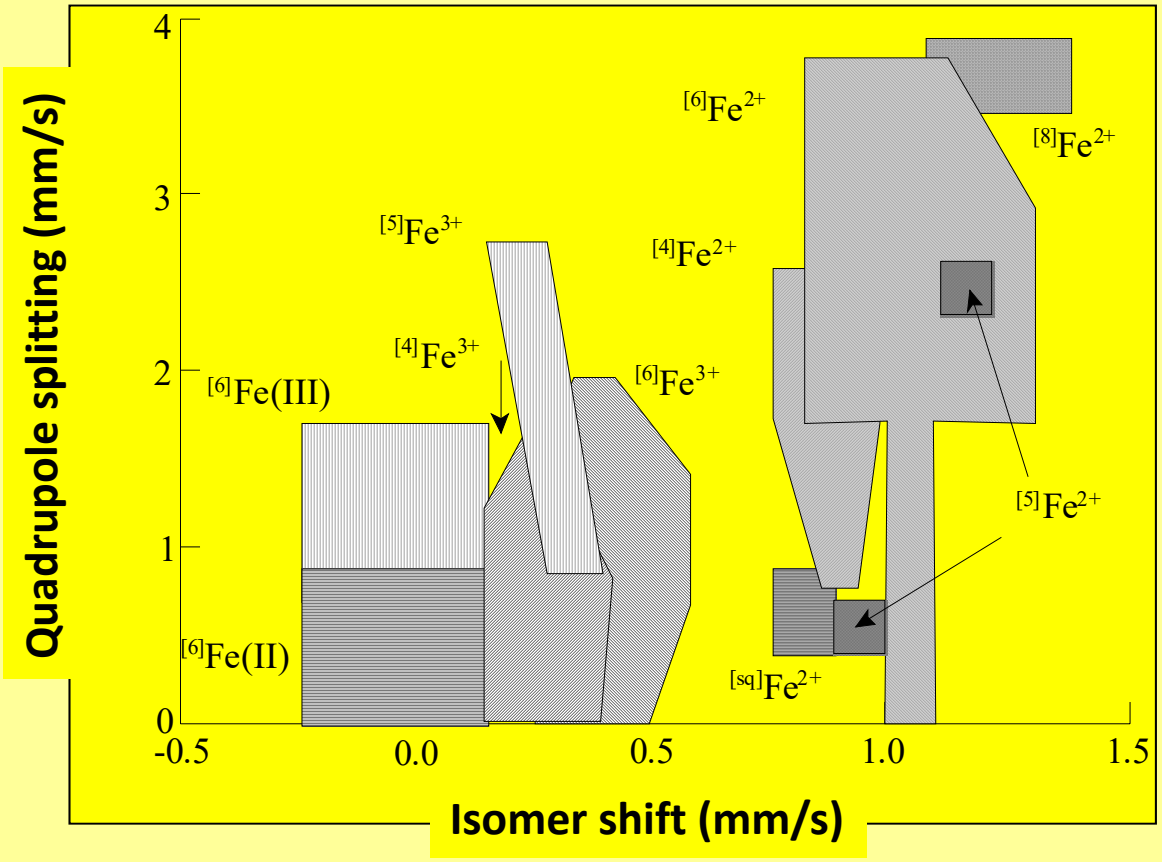


Fe(II)-LS the quadrupole splittings are rather small (0 to 0.8 mm/s)
Fe(III)-LS quadrupole splittings are larger (0.7 to 1.7 mm/s)

# Quadrupole Splitting $\Delta E_Q$ in $^{119}$Sn Mössbauer Spectra

**Sn(IV) Halides**

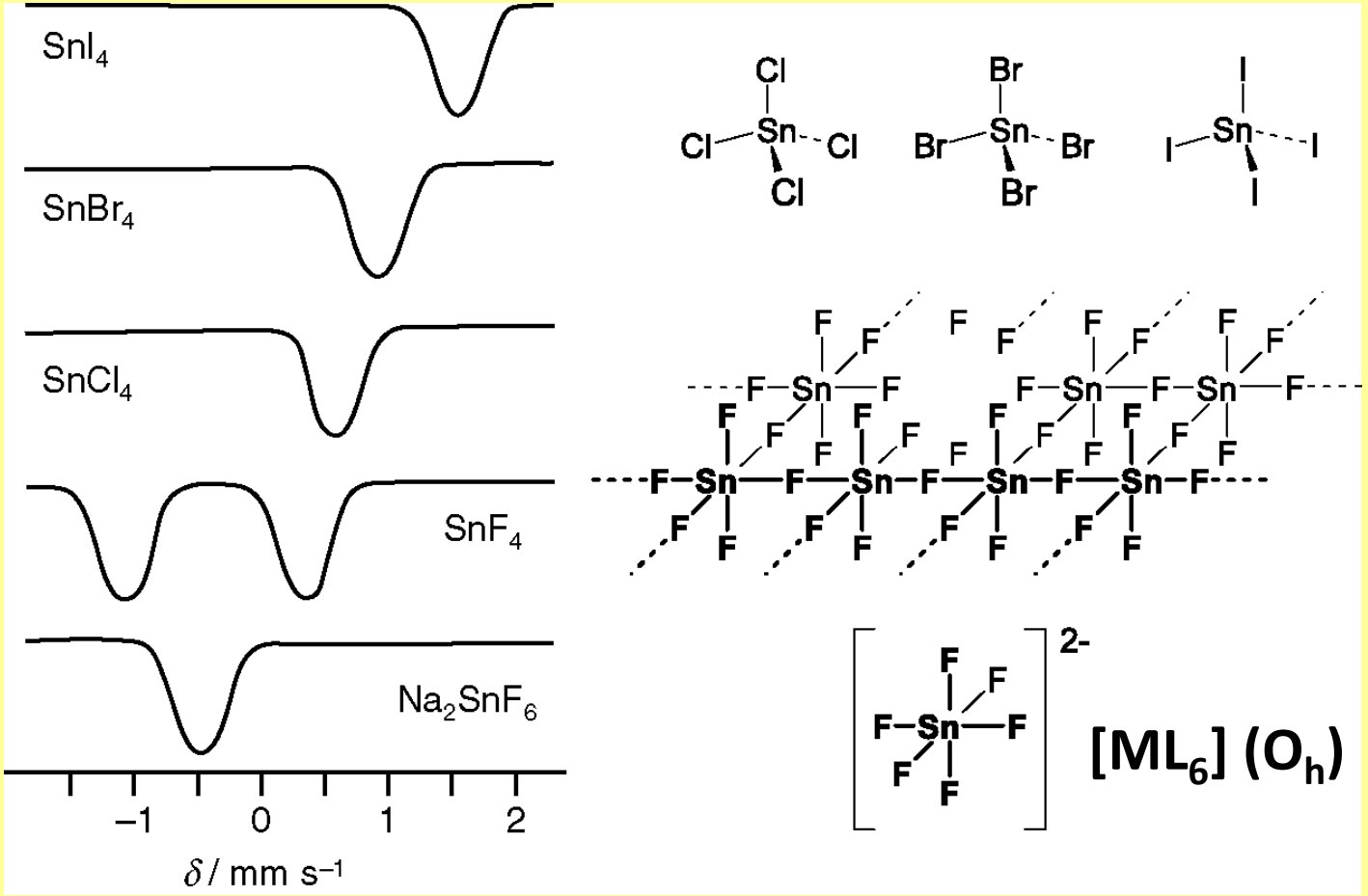

# Quadrupole Splitting $\Delta E_Q$ in $^{119}$Sn Mössbauer Spectra

$\Delta E_Q$

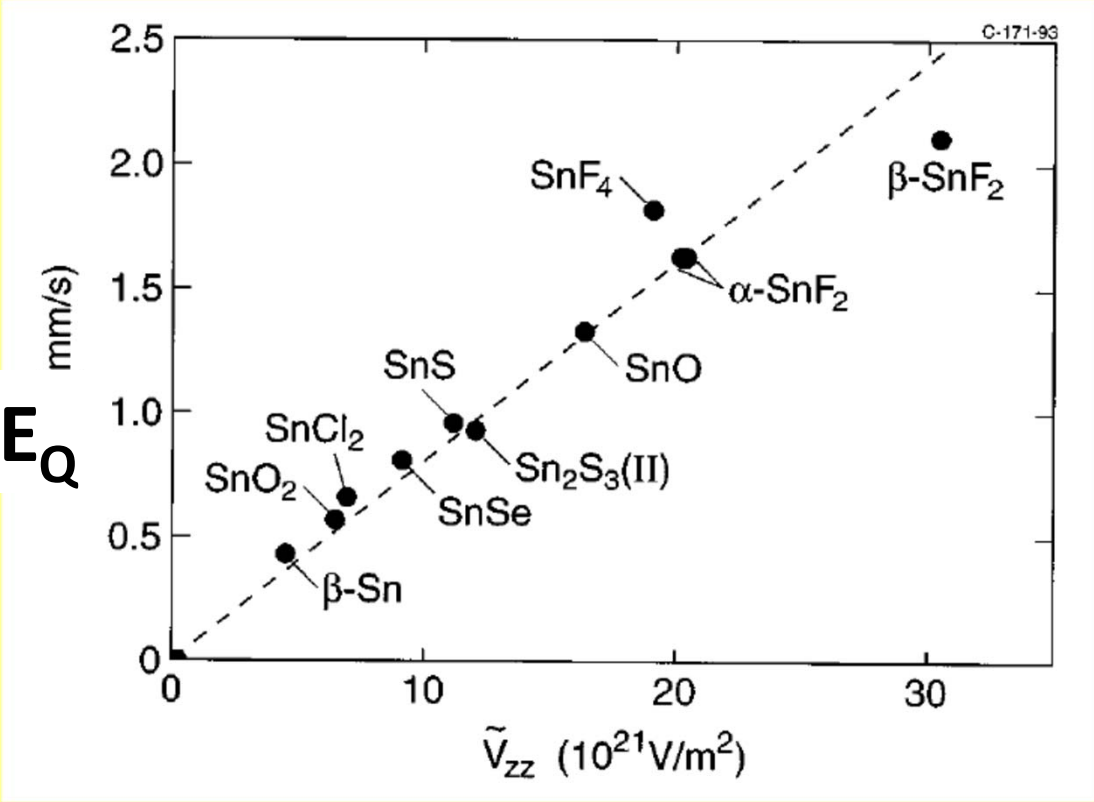


$$E_Q(I,m_I)=\frac{eQV_{zz}}{4I(2I-1)}\left[3m_I^2-I(I+1)\right]\left(1+\frac{\eta^2}{3}\right)^{\frac{1}{2}}$$

# Magnetic Dipole Interaction

**Hyperfine interactions**

***s*-electron densities** **EFG Quadrupole** **Magnetic field Magnetic dipole**

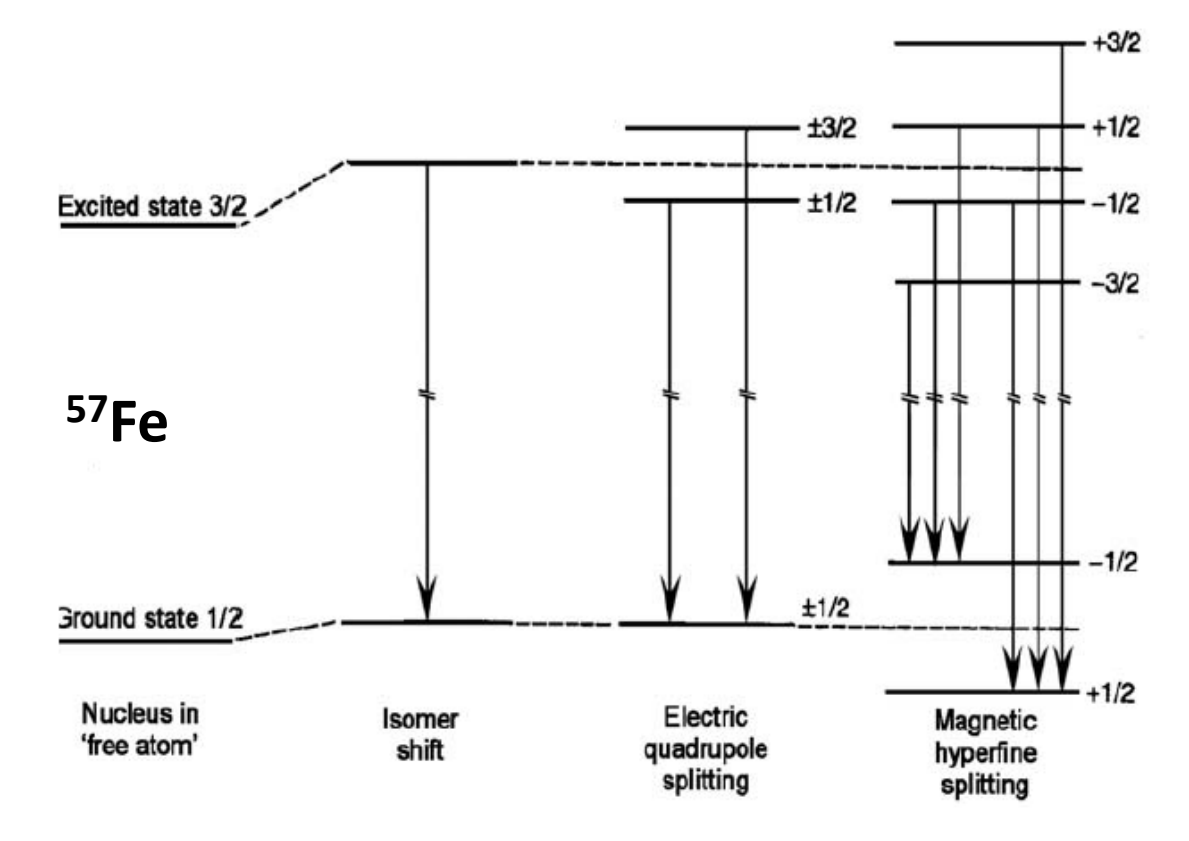

# Magnetic Dipole Interaction

Magnetic Field Splitting $\Delta E_M$

The requirements for magnetic dipole interaction

- the nuclear states involved possess **a magnetic dipole moment** $\mu$ ($I \geq ½$)
- **a magnetic field H** is present at the nucleus (ferro-, ferri-, or antiferromagnetic)

**$^{57}$Fe**

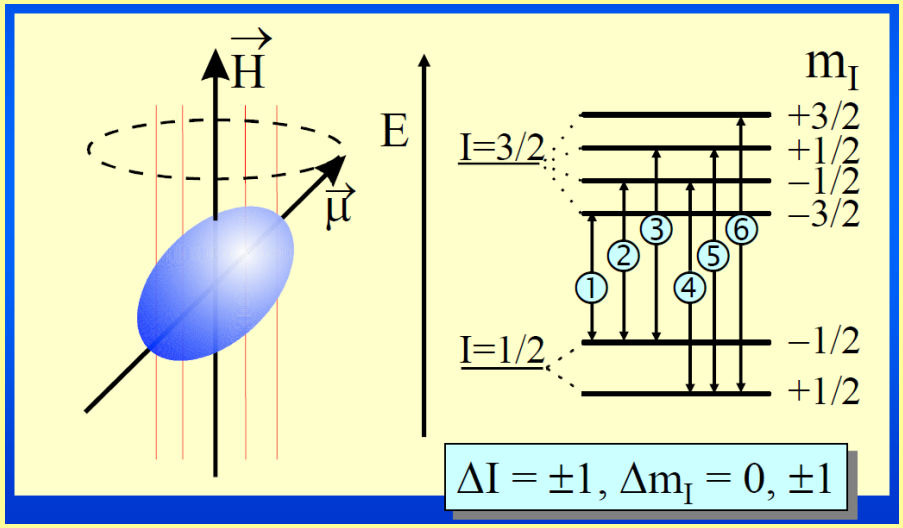


Magnetic dipole interaction = the precession of the magnetic dipole moment vector about the axis of the magnetic field

**Nuclear Zeeman splitting** of the states $I$, $m_I$ into $2I + 1$ substates (from $-I$ to $+I$)

# Magnetic Dipole Interaction

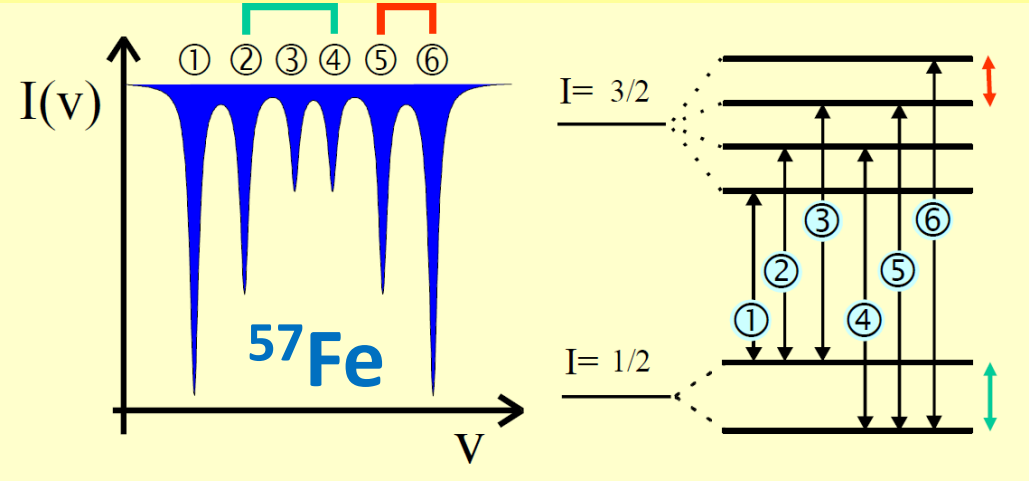


**Selection rules**

**$\Delta I = \pm 1$, $\Delta m_I = 0, \pm 1$**

The energies of the sublevels :

$$E_M(m_I) = -\mu H m_I / I = -g_N \beta_N H m_I$$

$g_N$ = the nuclear Landé factor, $\beta_N$ = the nuclear Bohr magneton

The separation between the lines 2 and 4 (also between 3 and 5) refers to the magnetic dipole splitting of the ground state

The separation between lines 5 and 6 (also between 1 and 2, 2 and 3, 4 and 5) refers to the magnetic dipole splitting of the excited $I = 3/2$ state

# Internal Magnetic Field

A hyperfine magnetic field $H_{int}$ (r = 0) at the nucleus can originate in various ways:

$$\mathbf{H_{int} = H_{Lat} + H_{FC} + H_{Dip} + H_{Orb} + H_{Ext}}$$ = total internal magnetic field

**Lattice magnetization $H_{Lat}$**
the magnetic field from the lattice magnetization (3d electrons), *M*, $H_{Lat} = 4\pi M/3$

**Fermi Contact Interaction $H_{FC}$**
the interaction of a nucleus and an **unpaired electron density**
Electron spin S of valence 3d-shell (e.g., S = 5/2 of $Fe^{3+}$) polarizes the 1s and 2s-electron density at the nucleus: **core polarisation**

s-electron spin density $|\Psi(0)\downarrow|^2 > |\Psi(0)\uparrow|^2$ magnetic field $H_{FC} \neq 0$

**Spin dipolar interaction $H_{Dip}$**
The magnetic moment of the electron spin at neighbouring atoms gives rise to dipolar interaction with the nucleus and causes a field at r = 0
Vanishes in cubic symmetry

# Internal Magnetic Field

**Orbital dipolar interaction $H_L$**

Electrons with orbital moment $L \neq 0$ give rise to an orbital magnetic moment accompanied by a magnetic field $\mathbf{H_L = -2\,\mu_B \langle r^{-3} \rangle \langle L \rangle}$

$\langle L \rangle$: expectation value of orbital angular momentum

**Externally applied field $H_{ext}$**

By applying an external magnetic field of known magnitude and direction one can determine the size and the direction of the intrinsic magnetic field of the material under investigation

# Combined Magnetic Dipole and Electric Quadrupole Interactions

$^{57}$Fe

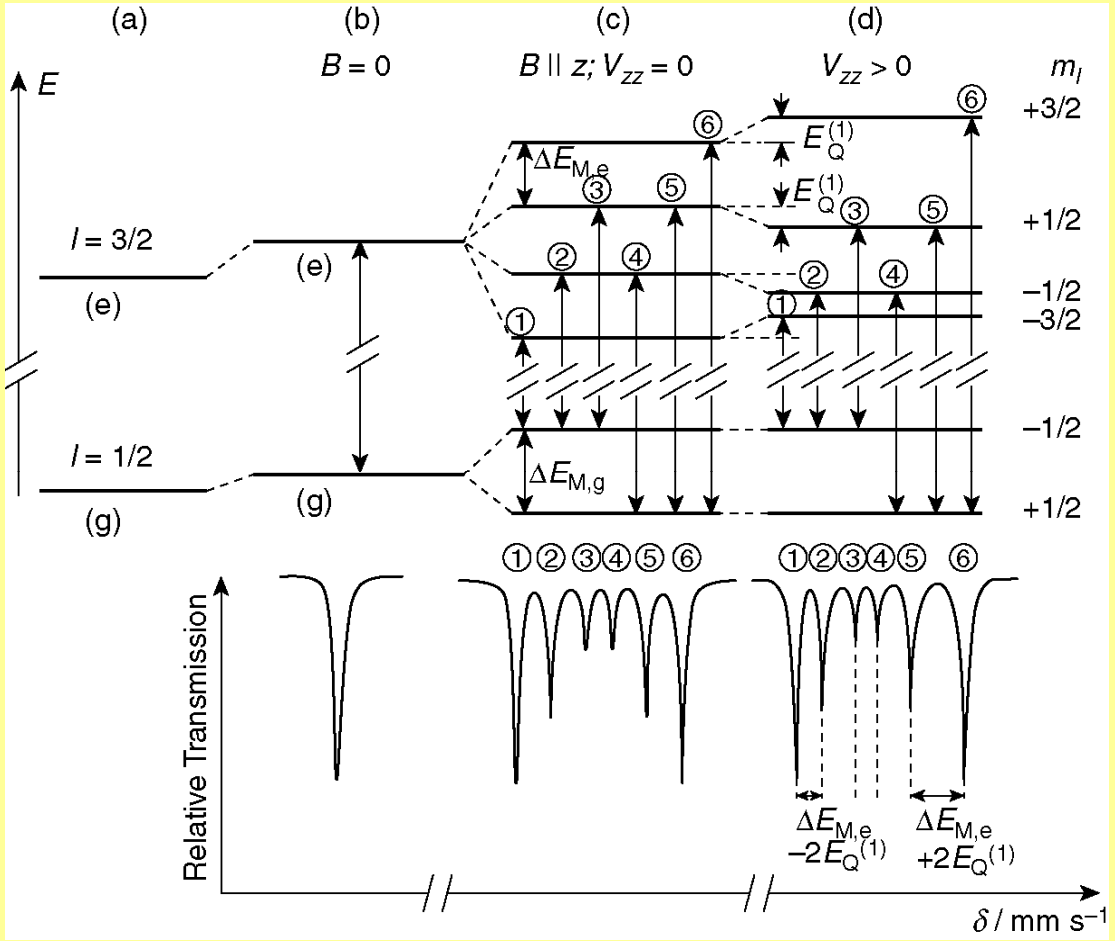


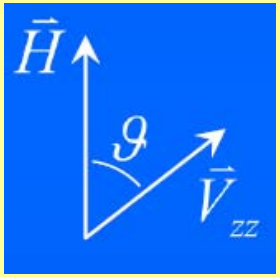


$$E_{M,Q}(I,m_I) = -g_N\beta_N H m_I + (-1)^{|m_I|+1/2}(eQV_{zz}/8)(3\cos^2\vartheta - 1)$$

# Combined Magnetic Dipole and Electric Quadrupole Interactions

**Magnetic dipole** interaction and **electric quadrupole** interaction may be present in a material simultaneously (together with the **electric monopole** interaction which is always present)

Relatively weak quadrupole interaction

The nuclear sublevels $I,m_I$ arising from magnetic dipole splitting are additionally shifted by the quadrupole interaction energies $E_Q(I,m_I)$

The sublevels of the excited $I = 3/2$ state are no longer equally spaced, the shifts by $E_Q$ are upwards or downwards depending on the direction of the EFG

This enables one to determine the sign of the quadrupole splitting parameter $\Delta E_Q$

The quadrupole shift parameter $\varepsilon$ depends on the canting angle $\varphi$ of the spins with respect to the electric field gradient (*E*Q) axis [111]
$\varepsilon = \Delta E_Q(3\cos^2\varphi - 1)/2$ and thus yields values with opposite sign for AF ($\varphi = 0°$) and WF ($\varphi = 90°$) states

# $^{57}$Fe Mössbauer Spectra

$^{57}$Fe

## Appearance of Mössbauer spectra

Depending on the local environments of the Fe atoms and the magnetic properties, Mössbauer spectra of iron oxides can consist of a singlet, a doublet, or a sextet.

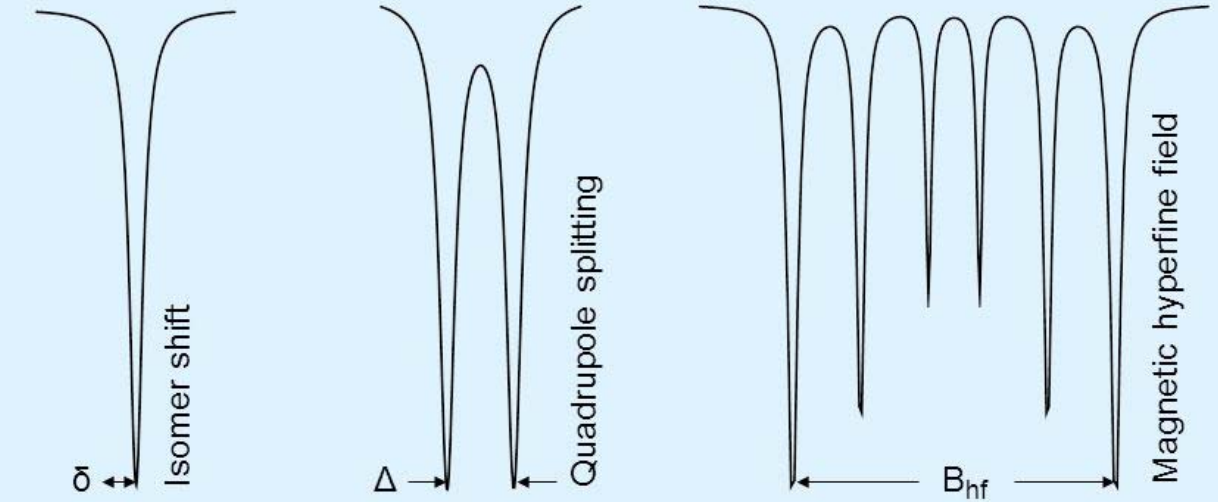


Symmetric charge
No magnetic field

Asymmetric charge
No magnetic field

Symmetric or asymmetric charge
Magnetic field (internal or external)

# $Fe_3(CO)_{12}$

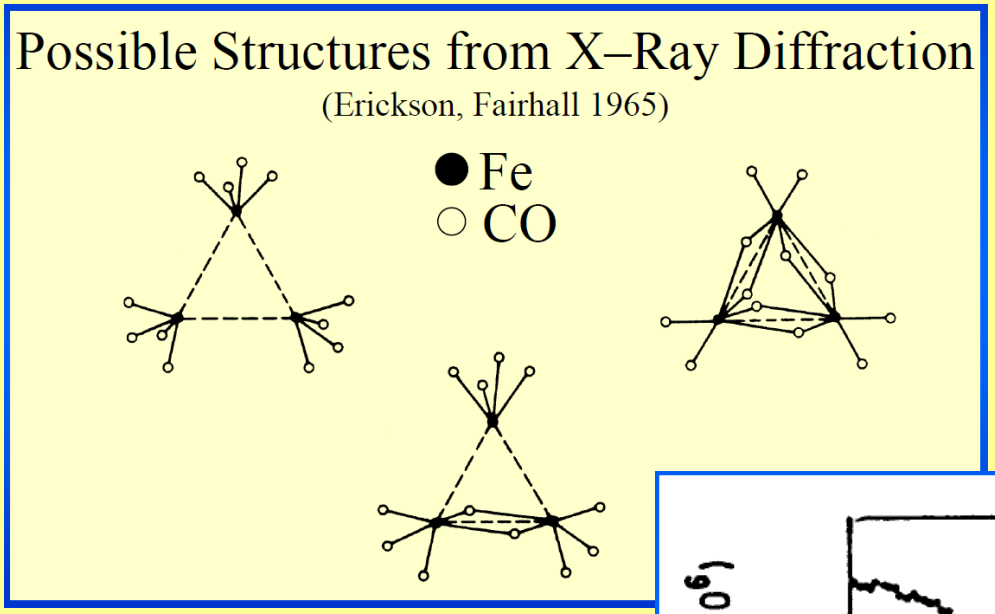
Possible Structures from X–Ray Diffraction
(Erickson, Fairhall 1965)
Fe
CO

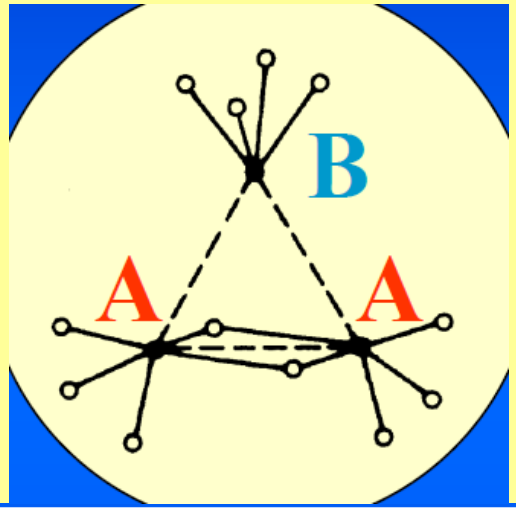
B
A
A

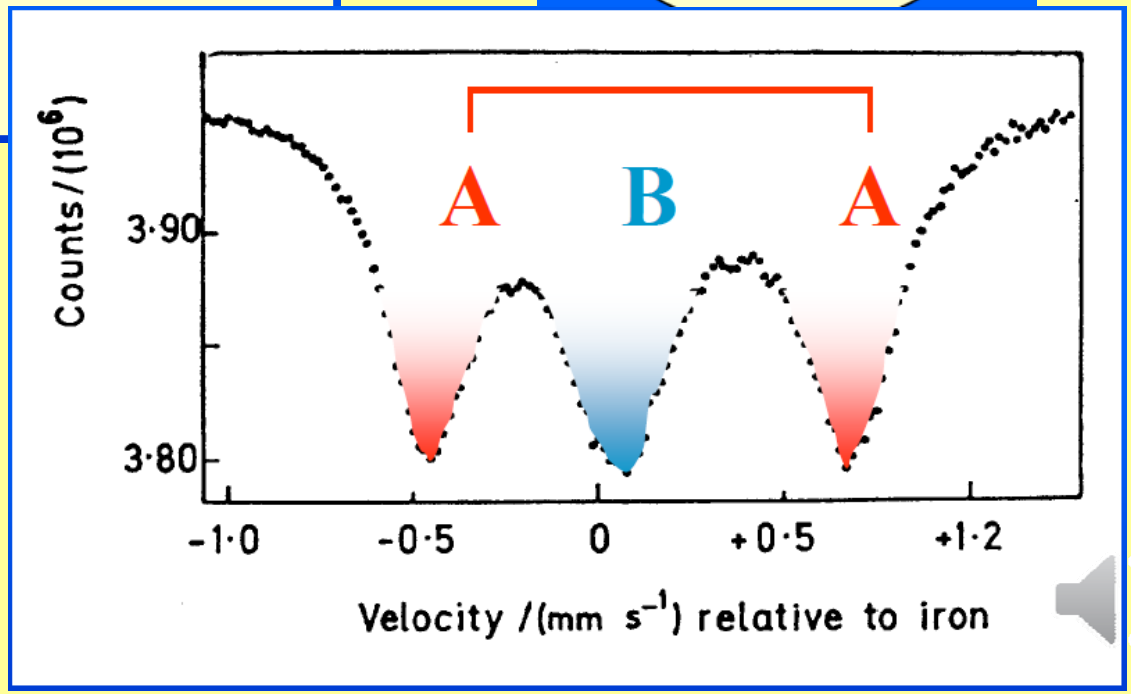
Counts / ($10^6$)
3·90
3·80
A
B
A
-1·0
-0·5
0
+0·5
+1·2
Velocity /(mm $s^{-1}$) relative to iron

# $[Fe_3(\mu_3\text{-}O)(OAc)_6(H_2O)_3]$

Variable-temperature $^{57}Fe$ Mössbauer spectra

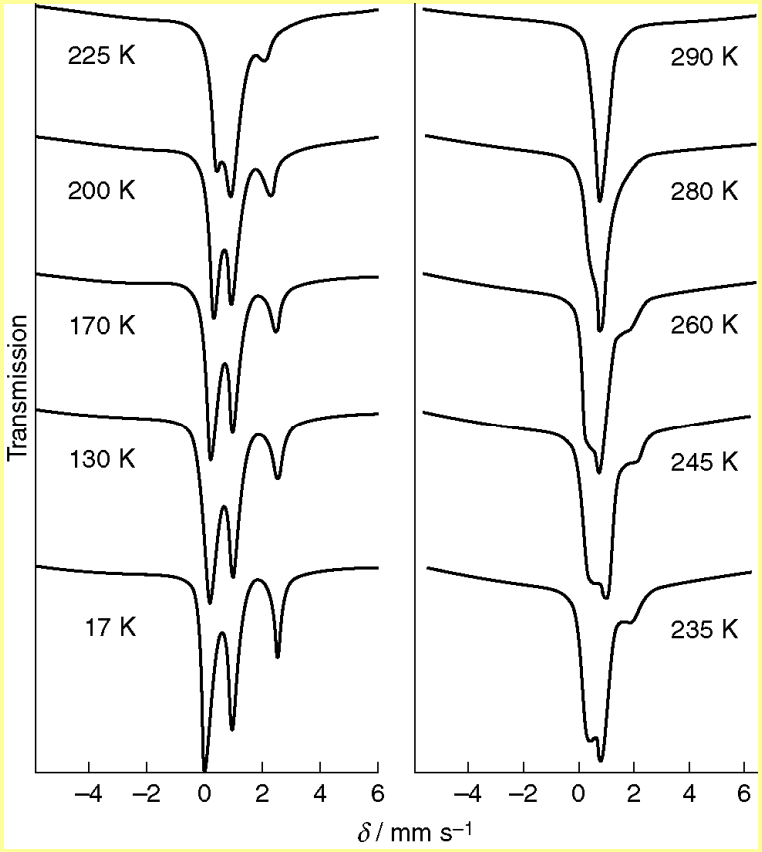


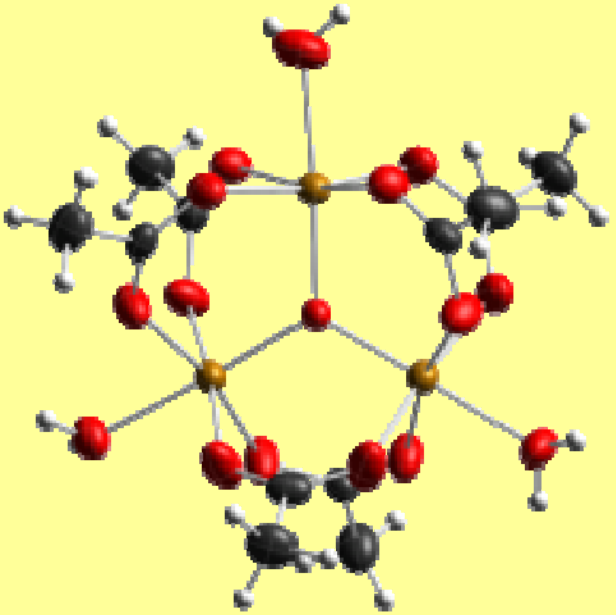

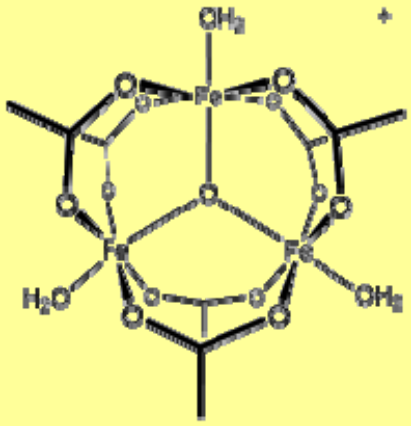

# $[Fe_3(\mu_3\text{-}O)(OAc)_6(3\text{-}Et\text{-}py)_3]\bullet S$

Variable-temperature $^{57}Fe$ Mössbauer spectra

**S = $CH_3CCl_3$**

"$Fe^{2.67+}$"

$Fe^{3+}$-HS

$Fe^{2+}$-HS

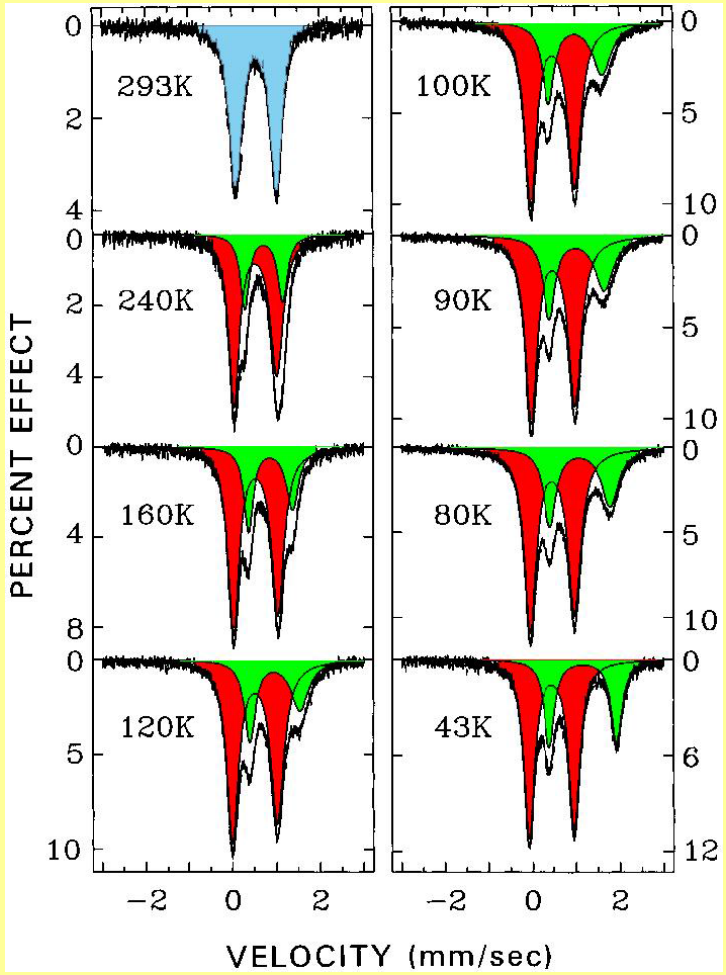


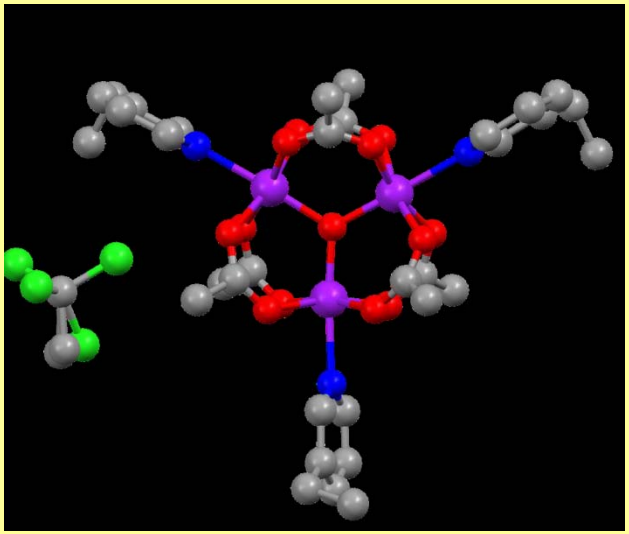

**$CH_3CCl_3$** - valence-trapped at low temperature, the ratio of the area fractions of Fe(III) to Fe(II) is close to 2 at low temperatures

Increasing temperature leads to valence detrapping near room temperature

# $[Fe_3(\mu_3\text{-}O)(OAc)_6(3\text{-}Et\text{-}py)_3]\bullet S$

Variable-temperature $^{57}Fe$ Mössbauer spectra

## S = $C_6H_6$ $CH_3CN$

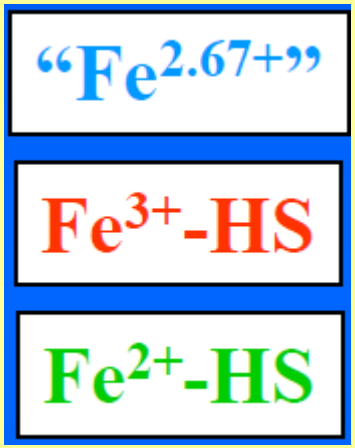


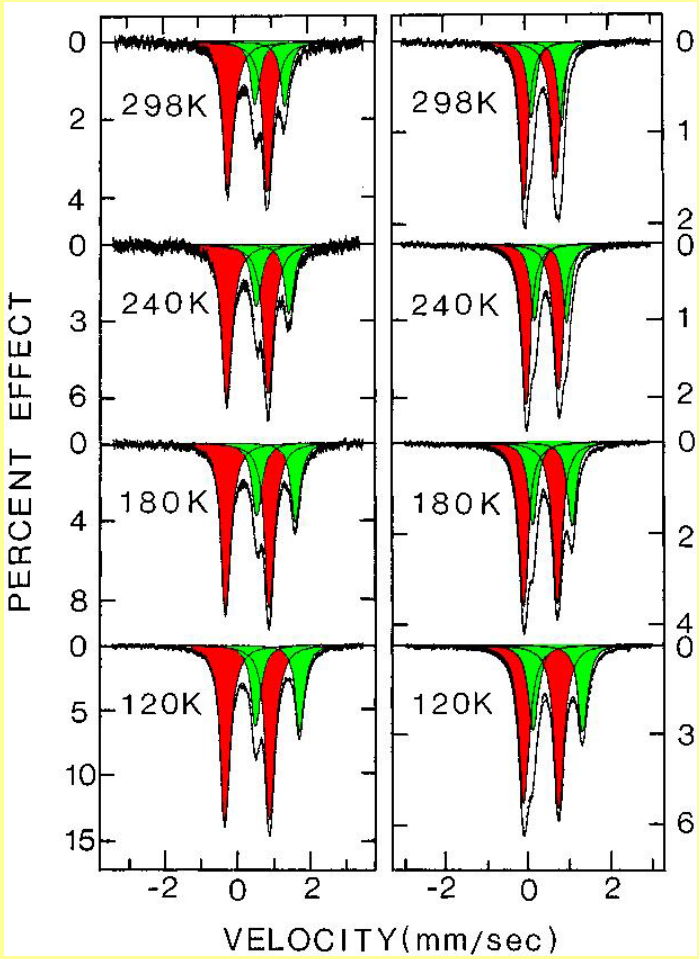


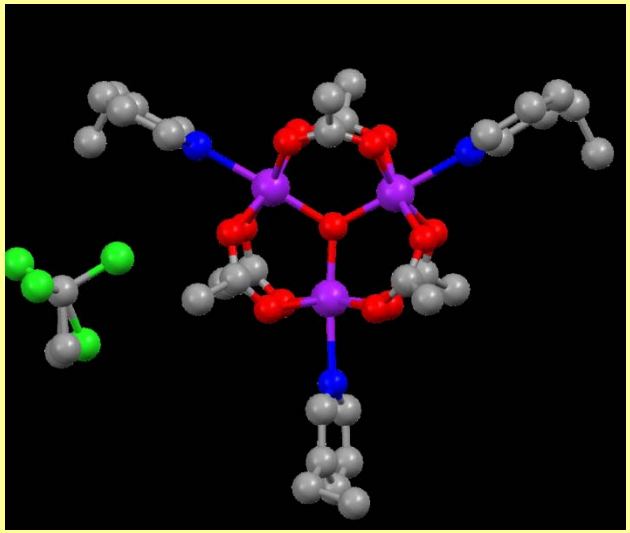

**$C_6H_6$** - valence-trapped from 120 to 298 K on the Mössbauer time scale (given by the lifetime of the nuclear excited state)

**$CH_3CN$** - increasing temperature leads to valence detrapping near room temperature

The lattice packing controls valence de/trapping

$C_6H_6$ - a stack type structure with strong intermolecular interactions due to overlapping py ligands, $C_6H_5CN$ and $CH_3CCl_3$ are layered

# γ-Radiolysis of $FeSO_4 \cdot 7H_2O$ (300 K)

$^{57}$Fe Mössbauer spectra

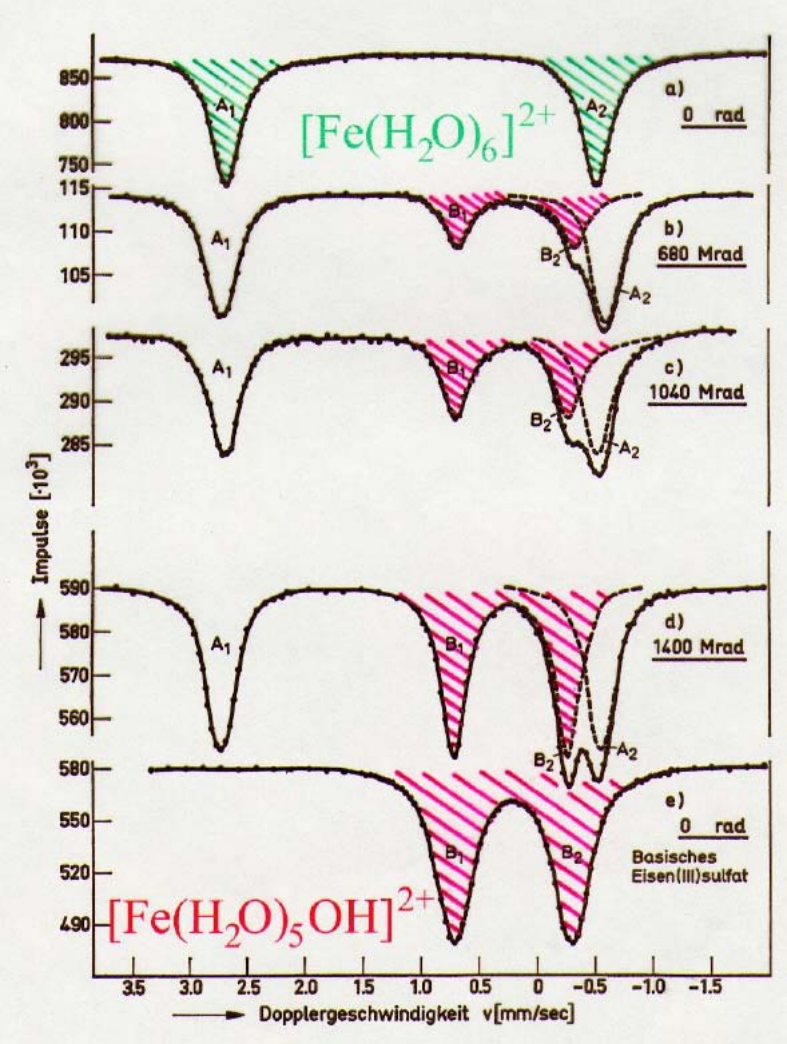


$$H_2O \rightsquigarrow H\bullet + \bullet OH$$

$$[Fe^{II}(H_2O)_5(\bullet OH)]^{2+} \rightarrow [Fe^{III}(H_2O)_5OH]^{2+}$$

# Fe Corrosion Products

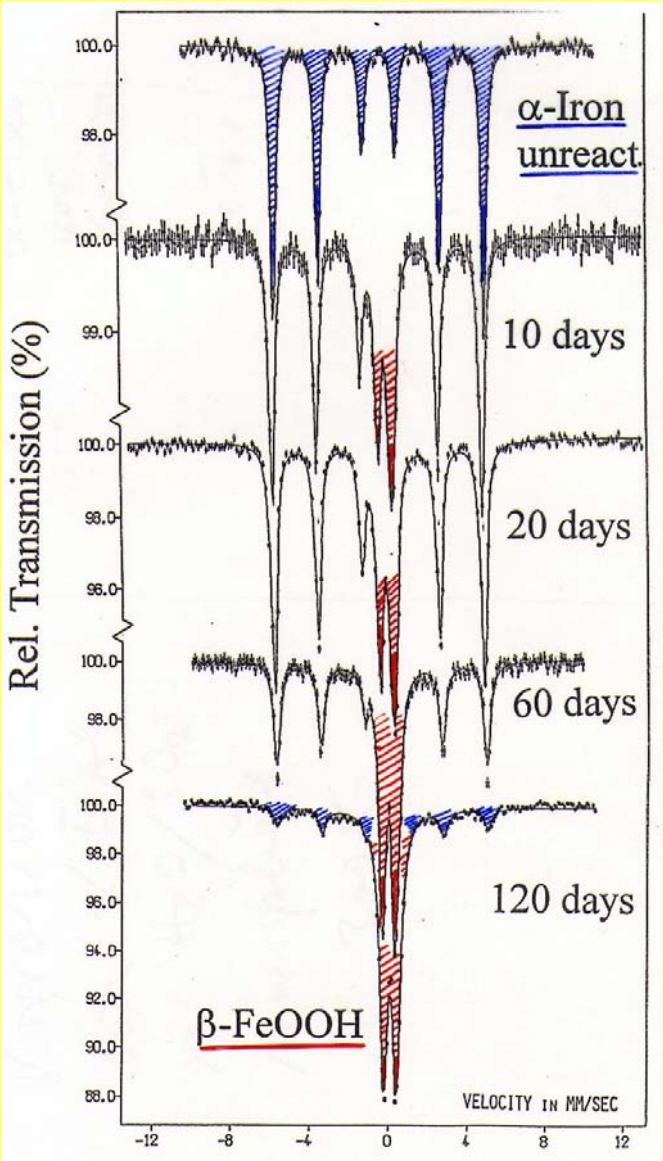


Corrosion of α-Iron
in $H_2O/SO_2$ atmosphere at 300 K

Corrosion product is β-FeOOH

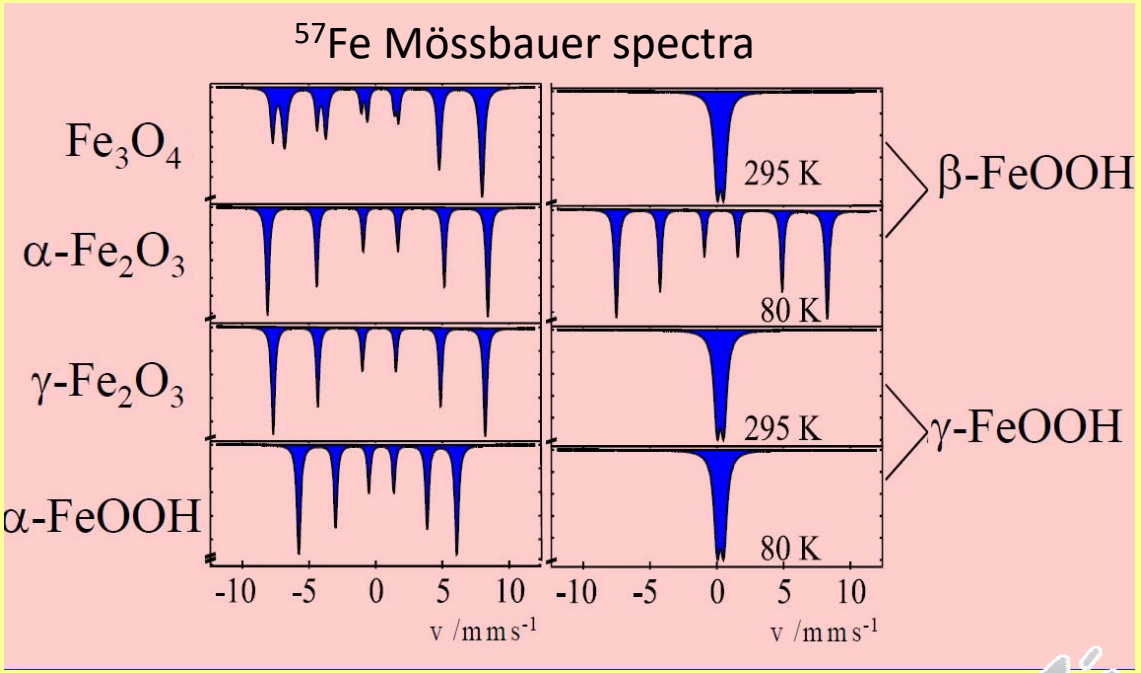

# Iron(III) Oxides

$^{57}$Fe Mössbauer spectral parameters

| iron(III) oxide phase | temperature [K] | Fe site | $IS_{Fe}$ [mm/s] | $QS/\varepsilon_Q$ [mm/s] | B [T] |
|---|---|---|---|---|---|
| $\alpha$-$Fe_2O_3$ Hematite | 300 | | 0.37 | -0.21 | 51.7 |
| | 4.2 | | 0.47 | 0.40 | 53.2 |
| $\beta$-$Fe_2O_3$ | 300 | d | 0.37 | 0.69 | - |
| | | b | 0.37 | 0.90 | - |
| | 15 | d | 0.50 | 0.23 | 47.9 |
| | | b | 0.47 | 0.77 | 50.6 |
| $\gamma$-$Fe_2O_3$ Maghemite | 300 | A | 0.27 | 0 | 48.8 |
| | | B | 0.41 | 0 | 49.9 |
| | 4.2 | A | 0.34 | 0 | 48.1 |
| | | B | 0.49 | 0 | 51.0 |
| $\varepsilon$-$Fe_2O_3$ | 300 | $Fe_1$ | 0.37 | -0.19 | 45.0 |
| | | $Fe_2$ | 0.39 | -0.06 | 45.2 |
| | | $Fe_3$ | 0.38 | 0 | 39.5 |
| | | $Fe_4$ | 0.21 | -0.07 | 26.3 |
| amorphous-$Fe_2O_3$ | 300 | | 0.34 | 0.78 | - |
| | 25 | | 0.47 | -0.03 | 46.8 |

$IS_{Fe}$ – isomer shift related to metallic iron, QS – quadrupole splitting for doublet spectrum, $\varepsilon_Q$ – quadrupole shift for sextet spectrum, B – hyperfine magnetic field

# Iron(III) Oxides

$^{57}$Fe Mössbauer spectra

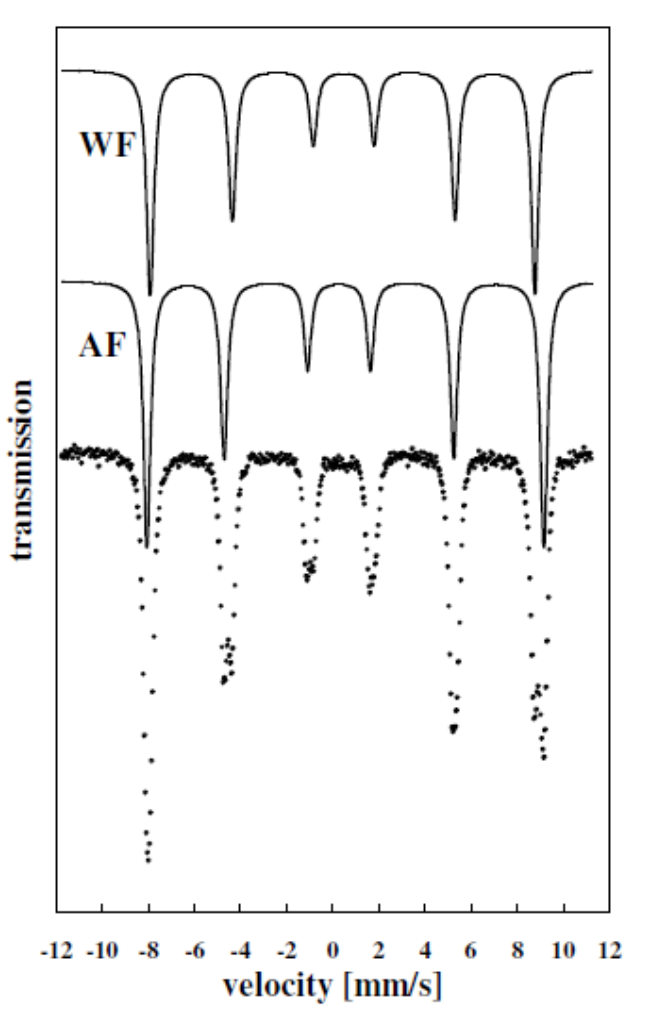


$\alpha$-$Fe_2O_3$ measured at 260 K near Morin transition temperature

**Hematite**
**$\alpha$-$Fe_2O_3$**
**(corundum)**

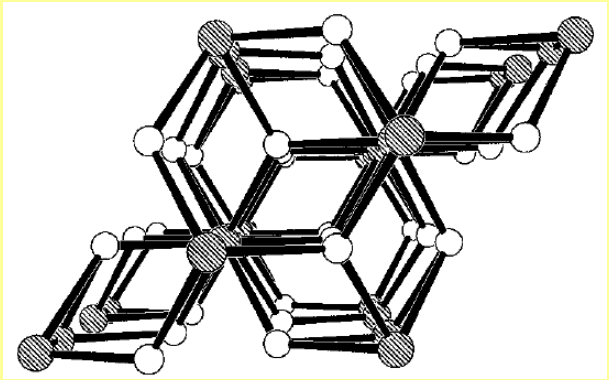

At T < 260 K - antiferromagnetic (AF) with the spins oriented along the electric field gradient axis

At Morin temperature ($T_M$), around 260 K, a reorientation of spins by about 90°, the spins become slightly canted to each other (by 5°), causing the destabilization of their perfect antiparallel arrangement = weak (parasitic) ferromagnetism (WF) between Morin and Neel temperature ($T_N$)

Above the Neel temperature of 950 K, hematite loses its magnetic ordering and is paramagnetic

# Iron(III) Oxides

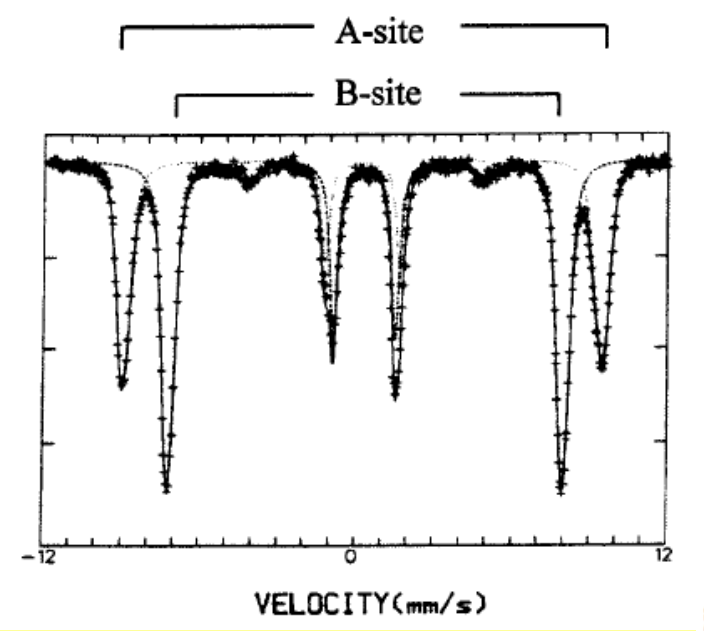


Mössbauer spectrum of a well-crystallized $\gamma$-$Fe_2O_3$ at 4 K in an external field of 6 T

## Maghemite $\gamma$-$Fe_2O_3$ (spinel)

ferrimagnetic

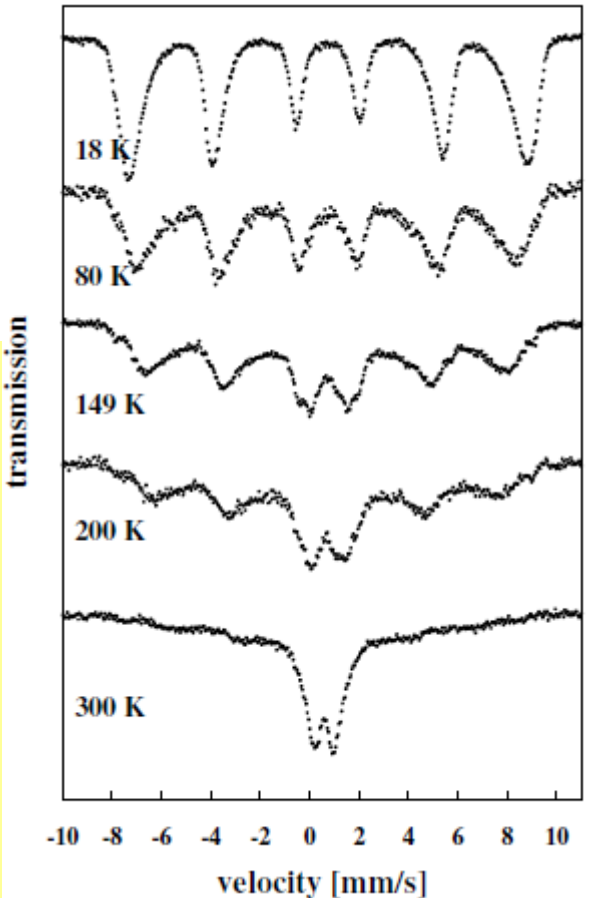


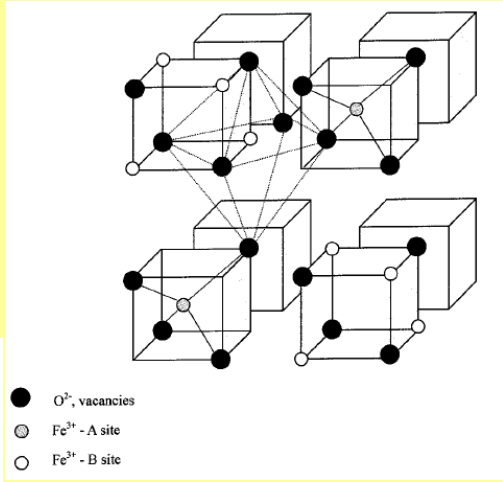


Cation-deficient inverse spinel structure

$$\left(Fe^{3+}\right)^{A}\left[Fe^{3+}_{5/3}\circ_{1/3}\right]^{B}O_4,$$

$$\left(Fe^{3+}_{8}\right)^{A}\left[\left(Fe^{3+}_{4/3}\circ_{8/3}\right)Fe^{3+}_{12}\right]^{B}O_{32},$$

# Iron in French Red Wine

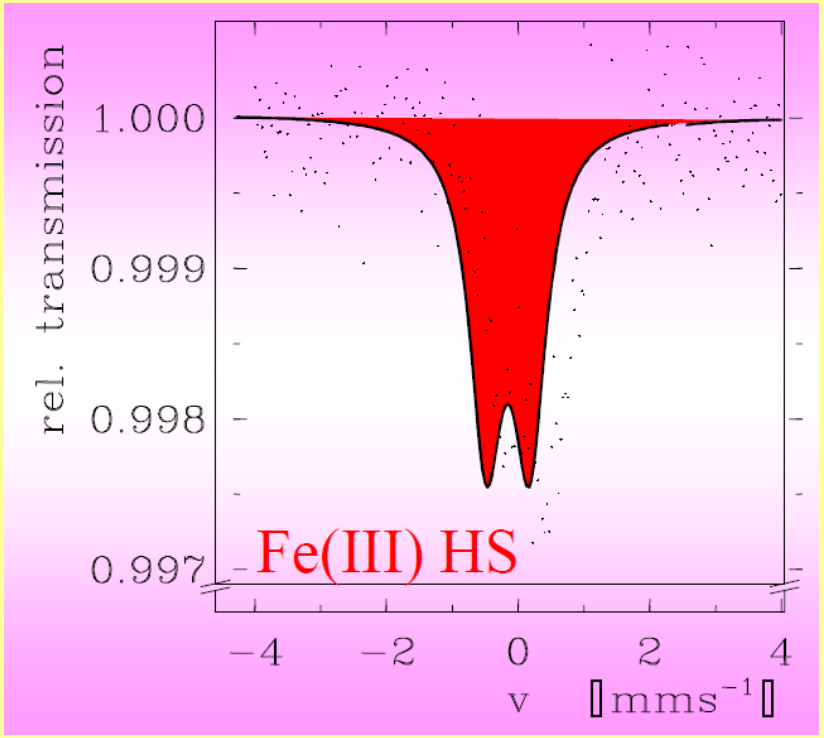

# Dictionary of Used Terms

Recoil – zpětný ráz
Halflife – poločas rozpadu
Orbital angular momentum – orbitální moment hybnosti